GLIA 56:394–411 (2008)

The ANP-cGMP-Protein Kinase G Pathway Induces a Phagocytic Phenotype but Decreases Inflammatory Gene Expression in Microglial Cells

MARIELA SUSANA BORÁN,[1] MARÍA ANTONIA BALTRONS,[1,2] AND AGUSTINA GARCÍA[1,2]*
[1]*Institute of Biotechnology and Biomedicine, Universidad Autónoma de Barcelona, Bellaterra, Barcelona, Spain*
[2]*Department of Biochemistry and Molecular Biology, Universidad Autónoma de Barcelona, Bellaterra, Barcelona, Spain*

KEY WORDS
actin; Rho GTPases; NOS-2; TNF-α; glia

ABSTRACT
Reactive gliosis is a prominent feature of CNS injury that involves dramatic changes in glial cell morphology together with increased motility, phagocytic activity, and release of inflammatory mediators. We have recently demonstrated that stimulation of the cGMP-protein kinase G (PKG) pathway by NO or atrial natriuretic peptide (ANP) regulates cytoskeleton dynamics and motility in rat astrocytes in culture. In this work, we show that the cGMP-PKG pathway stimulated by ANP, but not by NO, regulates microglial cell morphology by inducing a dramatic reorganization in the actin cytoskeleton. Both ANP (0.01–1.0 μM) and the permeable cGMP analog, dibutyryl-cGMP (1–100 μM), promote a rapid (maximal at 30 min) and concentration-dependent increase in size, rounding, and lamellipodia and filopodia formation in rat brain cultured microglia. These morphological changes involve an augment and redistribution of F-actin and result in increased phagocytic activity. ANP-induced rearrangements in actin cytoskeleton and inert particle phagocytosis are prevented by the PKG inhibitor, Rp-8-Br-PET-cGMPS (0.5 μM), and involve inhibition of RhoA GTPase and activation of Rac1 and Cdc42. However, ANP does not induce NO synthase Type 2 (NOS-2) or tumor necrosis factor-α expression and is able to decrease lipopolysaccharide (LPS)-elicited induction of these inflammatory genes. The morphological changes and the decrease of LPS-induced NOS-2 expression produced by ANP in cultured microglia are also observed by immunostaining in organotypic cultures from rat hippocampus. These results suggest that stimulation of the ANP-cGMP-PKG pathway in microglia could play a beneficial role in the resolution of neuroinflammation by removing dead cells and decreasing levels of proinflammatory mediators.

INTRODUCTION

Microglial cells, resident macrophages of the CNS, are able to participate in the innate immunity as phagocytes by removing dead cells and other debris and also as regulating cells under nonspecific inflammation conditions. Moreover, they can regulate functions of the adaptive immunity such as antigen presentation (Aloisi, 2001; Kim and de Vellis, 2005). In the normal brain, the so called resting microglial cells are highly ramified, with an elaborate tertiary and quaternary branch structure (Raivich et al., 1999). Although in their apparent resting state, microglial cells are greatly active, continually surveying their microenvironment with extremely motile processes and protrusions (Nimmerjahn et al., 2005). CNS injury provokes immediate and focal activation of microglia, switching their behavior from resting to defending cells in the injured site with a different response depending on the stimulation provided (Town et al., 2005). Reactive microglial cells proliferate and acquire an altered cellular morphology becoming larger and losing their enlarged cell processes. Concomitant with cellular hypertrophy, reactive microglia may release proinflammatory cytokines such as tumor necrosis factor-α (TNF-α) and interleukin-1β (IL-1β), and other inflammatory mediators (nitric oxide, arachidonic acid metabolites, reactive oxygen species) that can inhibit neurite outgrowth and affect cell survival (Kim and de Vellis, 2005). Thus, activated microglia have been implicated in several CNS pathologies including trauma, ischemia, and neurodegenerative diseases such as Alzheimer's and Parkinson's disease, multiple sclerosis, and HIV-associated dementia (Ghafouri et al., 2006; Kim and Joh, 2006; Streit, 2005; Wyss-Coray, 2006).

It is well-known from evidence in different cell types that the major molecular switches controlling actin cytoskeleton dynamics and thus cell morphology are the small GTP-binding proteins Rho GTPases, of which the three mayor members are RhoA, Rac, and Cdc42 (Etienne-Manneville and Hall, 2002; Hall, 1998). In macrophages, cells highly related to microglia, RhoA has been described to be involved in actin redistribution, whereas Rac has been shown to regulate the development of lamellipodia and membrane ruffles and Cdc42 the formation of filopodia at the cell periphery (Allen et al.,

This article contains supplementary material available via the Internet at http://www.interscience.wiley.com/jpages/0894-1491/suppmat.

Grant sponsor: Ministerio de Educación y Ciencia, Spain; Grant number: SAF2004-01717; Grant sponsor: Direcció General de Recerca (DGR); Grant sponsor: Generalitat de Catalunya; Grant number: SGR2001-212.

*Correspondence to: Agustina García, Instituto de Biotecnología y Biomedicina V. Villar Palasí, Universidad Autónoma de Barcelona, 08193, Bellaterra, Spain. E-mail: agustina.garcia@uab.es

Received 12 July 2007; Accepted 13 November 2007

DOI 10.1002/glia.20618

Published online 9 January 2008 in Wiley InterScience (www.interscience.wiley.com).

1997). In addition, the three Rho GTPases and their downstream effectors have been shown to play crucial roles during different types of phagocytosis (Caron and Hall, 1998; Cox et al., 1997; Leverrier and Ridley, 2001; Massol et al., 1998). Increasing evidence shows that cyclic GMP (cGMP) generated in response to NO or natriuretic peptides (NPs) regulates Rho GTPase activity and actin cytoskeleton dynamics in different cell types including macrophages (Begum et al., 2002; Boran and Garcia, 2007; Furst et al., 2005; Gudi et al., 2002; Ke et al., 2001; Krepinsky et al., 2003; Sandu et al., 2001; Sauzeau et al., 2000; Sawada et al., 2001). However, evidence of a similar role of cGMP in microglial cells is lacking.

Expression of inflammatory genes such as NO synthase Type 2 (NOS-2), TNF-α, or cyclooxigenase Type 2 (COX-2) can be up- or down-regulated in microglia by pro- or anti-inflammatory cytokines (Aloisi, 2001), neurotransmitters such as noradrenaline acting through the cyclic AMP-protein kinase A (cAMP-PKA) pathway (Dello Russo et al., 2004; Feinstein et al., 2002), contact with components of apoptotic cells (Minghetti et al., 2005) and P2 purinergic receptor activation (Potucek et al., 2006), among others. Numerous evidences support a role for cGMP-mediated pathways in the regulation of inflammatory gene expression in peripheral tissues with opposite effects depending on the cell type and the inflammatory stimulus (Pilz and Broderick, 2005; Vollmar, 2005). In vascular smooth muscle cells and cardiomyocytes, cGMP analogs and atrial natriuretic peptide (ANP) were shown to increase cytokine-induced expression of NOS-2, TNF-α, and COX-2 genes (Pilz and Broderick, 2005). Similarly, in mesangial cells cGMP amplifies NOS-2 and COX-2 mRNA transcription initially but leads to mRNA destabilization and decreased protein expression at later times (Diaz-Cazorla et al., 1999; Perez-Sala et al., 2001). In contrast, in macrophages the ANP-cGMP pathway has been shown to inhibit the lipopolysaccharide (LPS)-induced expression of NOS-2 and secretion of TNF-α by reducing the activation of NF-κB (Vollmar, 2005). In microglial cells, the available data are scarce and contradictory. Studies in the murine microglial cell line N9 suggested an anti-inflammatory role for cGMP since it was able to inhibit Aβ-amyloid-induced release of leukotriene B4 (Paris et al., 1999) and to reduce LPS-induced secretion of TNF-α (Paris et al., 2000). However, a more recent study in a different murine microglial cell line (BV2) showed that LPS-induced expression of the inflammatory gene CD11b is mediated by the NO-cGMP pathway (Roy et al., 2006). Contradictory results have also been reported using rat microglial cultures. Whereas Choi et al. (2002) observed that the cGMP-selective phosphodiesterase inhibitor zaprinast enhanced TNF-α and IL-1β secretion as well as NOS-2 and major histocompatibility complex class II molecule (MHC II) expression, Moriyama et al. (2006) described ANP inhibition of LPS-induced NO secretion and IL-1β expression.

In cultured astrocytes, we recently reported that both NO- and ANP-cGMP-protein kinase G (PKG) pathways regulate actin cytoskeleton dynamics by inactivation of RhoA (Boran and Garcia, 2007). In the course of this study, we observed that morphological changes and intense accumulations of F-actin occurred in response to cGMP analogs in the microglial cells contaminating the primary astrocyte cultures. This observation prompted us to perform this study. We report here that in rat microglial cells, stimulation of the cGMP-PKG pathway by ANP but not by NO, dramatically alters the microglial actin cytoskeleton by regulating Rho GTPase activity and promotes the acquisition of an amoeboid morphology that shows increased phagocytic activity. However, this phagocytic phenotype is not associated with induction of NOS-2 or TNF-α expression and furthermore ANP is able to decrease LPS-elicited expression of these proteins.

MATERIALS AND METHODS

Materials

Dulbecco's modified Eagle's medium (DMEM), penicillin, streptomycin, LPS (from *Salmonella typhimurium)*, ANP, dibutyryl-cyclic GMP (dbcGMP), sodium nitroprusiate (SNP), 3-isobutyl-1-methylxanthine (IBMX), paraformaldehyde, 1H-[1,2,4]oxodiazolo-[4,3-a]quinoxalin-1-one (ODQ), cytosine arabinoside (Cyt-ara), Triton X-100, methanol, bovine serum albumin (BSA), 4′,6-diamidino-2-phenylindole (DAPI), geranylgeranyl pyrophosphate (GGpp), phosphatase inhibitors, mouse anti-actin and anti-FLAG antibodies were obtained from Sigma. Rp-8Br-PET-cGMPS and Rp-cAMPS, PKG and PKA inhibitors, respectively were from Biolog Life Science Institute; fetal-calf serum (FCS) from Ingelheim Diagnóstica. ROCK (RhoA GTPase kinase) inhibitor Y-27632 was from Calbiochem. Rhodamine–phalloidin, BODIPY FL-phallacidin, tetramethylrhodamine-conjugated particles from *E. coli* (K-12 strain), red fluorescent inert particles (excitation/emission maxima = 580/608), acetylated low-density lipoprotein (Ac-LDL) labeled with 1,1′ dioctadecyl-3,3,3′,3′ tetramethylindocarbocyanine perchlorate (Dil-Ac-LDL) or with Alexa 488 (Alexa 488-Ac-LDL); Alexa 488, 555, or 568 coupled to anti-IgG secondary antibodies (from goat, donkey, or rabbit), horse serum and trypsin solution were from Invitrogen. C-type natriuretic peptide (CNP) was from NeoMPS. Sheep anti-cGMP antibody developed against paraformaldehyde-fixed cGMP linked to tiroglobulina was kindly donated by Dr. de Vente (Maastricht University, The Netherlands) and the corresponding secondary antibodies labeled with FITC or Cy3 were purchased from Amersham. Protease inhibitor cocktail was from Roche. Rabbit anti-NOS-2 and mouse anti-myc antibodies were from Santa Cruz Biotechnology. Mouse anti-CD68 and anti-CD11b antibodies were from Serotec. Anti-rat TNF-α antibody was from R&D Systems. Polyethyl-enimine (PEI, 25 kDa) was purchased from Polysciences. Plasmids pEXV3-V14RhoA-myc, pEXV3-N17Rac1-myc, and pCMV-N17Cdc42-FLAG were kindly donated by Drs. A. Ridley (UCL, London, UK) and C. Guerri (CIPF, Valencia, Spain).

Cultures

Primary cell cultures

Astrocyte-enriched cultures were prepared from cerebellum of 7-day-old Sprague–Dawley rats with little modifications of the method previously described (Agullo et al., 1995). In brief, rats were decapitated and cerebella immediately dissected out. After meninges and blood vessels were removed, the tissue was minced and incubated for 10 min at 37°C in Ca^{2+}-free Krebs–Ringer buffer containing 0.025% trypsin. Cells were then mechanically triturated through a glass pipette and filtered through a 40-μm nylon mesh in the presence of 0.52 mg/mL soybean trypsin inhibitor and 170 IU/mL DNase. After centrifugation (500*g*), cells in 90% DMEM, 10% FCS, 20 U/mL penicillin, and 20 μg/mL streptomycin, were seeded in 35-mm diameter plastic Petri dishes at 1.25×10^5 cells/cm^2. For immunofluorescence staining experiments, a 24 × 24 mm glass cover slip was inserted into each dish before seeding. Cells were maintained in a humidified atmosphere of 90% air–10% CO_2. Medium was changed once a week and cells were used after 14–19 days *in vitro* (14–19 DIV). These cultures that are enriched in astrocytes also contain microglial cells that show a drastic increase in number when the astrocyte monolayer reaches confluency (10 DIV) representing up to 20–30% of the total amount of cells at 14 DIV (Agullo et al., 1995). In some experiments, confluent cultures (10 DIV) were treated with Cyt-ara 10 μM until the day of use (14 DIV) to decrease microglial contamination (Agullo et al., 1995).

Microglial cultures were prepared by mild trypsinization of confluent astrocyte-enriched cultures as described by Saura et al. (2003). Briefly, once cultures reached confluency, monolayers were washed twice with DMEM and were incubated at 37°C with a trypsin solution—0.25% trypsin, 1 mM EDTA in Hank's buffered salt solution—diluted 1:4 in DMEM until the astrocyte monolayer detached (about 30 min); this medium was then aspirated and replaced with DMEM (serum free). Cells were maintained in this medium for at least 2 DIV. In these cultures, more than 98% of the cells are microglia as estimated by Dil-Ac-LDL and CD68 staining. Cells were treated with the different compounds in serum free-DMEM for the indicated times and concentrations.

Organotypic cultures

Hippocampal slice cultures were prepared according to established methods (Stoppini et al., 1991). Transverse sections (400 μm) of hippocampi from 7 to 8-day-old Sprague–Dawley rats were prepared using a McIlwain tissue chopper (Mickle Laboratory Engineering). Slices were plated onto Millicell-CM tissue culture inserts (four slices per insert, Millipore) and incubated with 5% CO_2 at 37°C for 10–12 days in a culture medium composed of 50% MEM, 25% heat-inactivated horse serum, 25% Hanks' solution buffered to pH 7.4 by addition of 5 mM Tris and 4 mM $NaHCO_3$, 6.5 mg/mL glucose, penicillin (10,000 U/100 mL), and streptomycin (1 mg/100 mL). The medium was changed after 24 h in culture and every 3–4 days subsequently.

F-Actin Staining and Quantification

After fixing with 4% paraformaldehyde in phosphate-buffered saline (PBS) (40 min, RT), cells were washed and incubated with 0.1% Triton X-100 in PBS for 3 min, then nonspecific binding was blocked with 1% BSA–PBS for 30 min. Next, cells were incubated overnight at 4°C with BODIPY FL-phallacidin or rhodamine–phalloidin (diluted 1:200 in 1% BSA–PBS) and washed several times. For F-actin double-stainings, the corresponding F-actin marker was added during the secondary antibody incubation. For F-actin/microglia staining, cultures were incubated with the microglial marker Dil-Ac-LDL (10 μg/mL, 4 h, 37°C) before fixation (see below). For F-actin quantification, cells were first stained for F-actin as above using rhodamine–phalloidin (incubated 1:200 in 1% BSA–PBS for 20 min at RT). Afterwards, cells were treated with methanol to extract the rhodamine–phalloidin bound to F-actin (4°C, 1 h with agitation) (Howard and Oresajo, 1985). This extract was measured with fluorescence emission at 595 nm and excitation at 531 nm using a Victor fluorescence plate reader (Wallac, Gaithersburg, MD). F-actin content per dish was determined in duplicates and four dishes were assayed for each treatment. The amount of F-actin per microgram of protein was expressed relative to untreated cells processed in parallel on the same day. Protein concentration was determined by the method of Bradford using BSA as standard.

Cell Staining

Microglia

To label microglia, cultures were incubated with the microglial marker Dil-Ac-LDL or Alexa 488-Ac-LDL (10 μg/mL, 4 h, 37°C), and then washed twice with PBS (pH 7.4).

cGMP

Cultures were washed and preincubated for 10 min at 37°C in PBS before stimulation with SNP (100 μM) or ANP (1 μM) for 3–120 min in the presence of 1 mM IBMX. Immediately after the incubation, cells were fixed with 4% paraformaldehyde in PBS (40 min, RT) and incubated in 0.1% Triton X-100 (15 min, RT). Nonspecific binding was blocked with 1% BSA–PBS for 30 min. Then, cells were incubated with sheep anti-cGMP antibody, diluted 1:4,000 in 0.1% BSA–PBS (de Vente et al., 1989). The primary antibody was omitted in controls. After washing, cultures were incubated for 1 h with Cy3- or FITC-conjugated anti-sheep IgG antibody (diluted 1:1,000 in 0.1% BSA–PBS at RT). For cGMP/microglia

double-staining, cGMP staining was performed after incubation with the microglial marker Alexa 488-Ac-LDL (10 μg/mL, 4 h, 37°C).

NOS-2

For microglia/NOS-2 staining in cell cultures, mouse CD68 antibody (1:500) was incubated together with rabbit anti-NOS-2 antibody (1:200), both in 0.1% PBS–BSA followed by Alexa 488 anti-rabbit IgG and Alexa 555 anti-mouse IgG (both diluted 1:1,000). For microglia/NOS-2 staining in organotypic cultures, slices were incubated for 48 h at 4°C with mouse anti-CD11b and rabbit anti-NOS-2 antibodies (1:500 and 1:200 in 0.1% BSA–PBS, respectively). After washing, slices were incubated overnight with goat Alexa 568 anti-mouse IgG and goat Alexa 488 anti-rabbit IgG antibodies (both 1:1,000 in 0.1% BSA–PBS at 4°C). Primary antibodies were omitted in controls. After cutting out the Millicell membrane, they were mounted and images captured using confocal microscopy.

TNF-α

Cultures fixed with 4% paraformaldehyde in PBS (40 min, RT) were incubated for 18 h at 4°C with anti-rat TNF-α antibody diluted 1:150 in 0.1% PBS–BSA followed by donkey Alexa 488 anti-goat IgG antibody (1 h, RT, diluted 1:1,000 in 0.1% PBS–BSA). For TNF-α/microglia double staining, anti-TNF-α antibody was incubated together with mouse anti-CD68 antibody (1:500) and then rabbit Alexa 568 anti-mouse IgG antibody (1:1,000) was added in the secondary antibody incubation.

Nuclei

In some experiments, DAPI (0.25 μg/mL) was added for nuclei labeling. Photomicrographs were digitally recorded with a Nikon (model Eclipse 90i) or a confocal Leica (model TSC SP2) microscope.

Cell Transfections

About 2–3 h before transfection, microglia cultures were changed to fresh DMEM–10% FCS. Plasmid DNAs were first diluted in serum-free DMEM in a volume equivalent to one-tenth of that in the culture to be transfected, then PEI was added to this suspension in a 1:10 DNA:PEI ratio. The mixture was immediately vortexed for 5 s, incubated for 10 min at RT, and added dropwise to the cells. Dishes were then incubated for 12 h, and afterwards the transfected mixture was removed by changing to fresh serum-free medium. After 10 h of incubation, vehicle or ANP 1 μM was added for 30 min or 2 h. Myc/F-actin or FLAG/F-actin double-stainings were performed using mouse anti-9E10 antibody (1:300) for c-myc detection or mouse anti-FLAG antibody (1:1,000). Rhodamine–phalloidin was added during the secondary antibody incubation for myc or FLAG detection.

Phagocytosis Assay

To study microglial phagocytic capacity, fluorescent *E. coli* or inert particles/F-actin double-staining was performed. Microglial cultures were treated with 0.1 mg/mL of particles in the presence or absence of ANP (1 μM), dbcGMP (100 μM), GGpp (10 μM), Y-27632 (20 μM), or combinations between them, and incubated for 30 min at 37°C. Controls for nonspecific binding were incubated in parallel at 4°C. In some experiments, cultures were pretreated with the PKG inhibitor Rp-8Br-PET-cGMPS (0.5 μM, 1 h) or with the RhoA kinase (ROCK) inhibitor Y-27632 (20 μM, 10 min when used in combination with ANP). Cells were washed several times and F-actin was stained as earlier. Photomicrographs were taken and analyzed by confocal microscopy to differentiate between truly internalized versus externally membrane-bound particles. To perform this, approximately 15 sections of 0.4–0.5 μm were taken between the upper and lower cell edges and then analyzed with Leica TSC2 Software. In 4°C controls, 96% of the particles in contact with cells were membrane-associated in ANP-challenged cultures, whereas a similar percentage of particles were truly internalized at 37°C after that treatment (Supplementary Fig. 1). For routine experiments, photomicrographs were digitally recorded with a Nikon (model Eclipse 90i) microscope. F-actin labeling and fluorescence particles of the same fields were merged and the amount of *E. coli* or inert particles/cell was counted in at least 100 cells per treatment in each of three different experiments.

Western Blot

To determine NOS-2 protein levels, cell cultures previously treated with LPS (100 ng/mL), ANP (1 μM), or both for 24 h, were homogenized in ice-cold 50 mM Tris/HCl 1 mM EDTA buffer (pH 7.4 at 37°C), containing antiprotease cocktail and phosphatase inhibitors with a glass-Teflon Potter-Elvehjeim homogenizer (20 strokes, mechanically driven at 800 rpm). Equal amounts of protein (30 μg) were subjected to SDS-PAGE, transferred to polyvinyl difluoride membranes, and probed with mouse anti-NOS-2 (1:1,000) and anti-actin (1:125,000) primary antibodies. This step was followed by incubation with anti-mouse IgG-horseradish peroxidase-labeled secondary antibody (1:4,000) and subsequent detection with an enhanced chemiluminescence detection kit (Biological Industries).

Measurement of TNF-α

TNF-α levels were determined in the culture media by a bead-based immunoassay commercial kit according to manufacturer's instructions (BD Biosciences) using a flow cytometer (FACSCanto, BD Biosciences). Data were analyzed by FCAP Array™ Software (BD Biosciences).

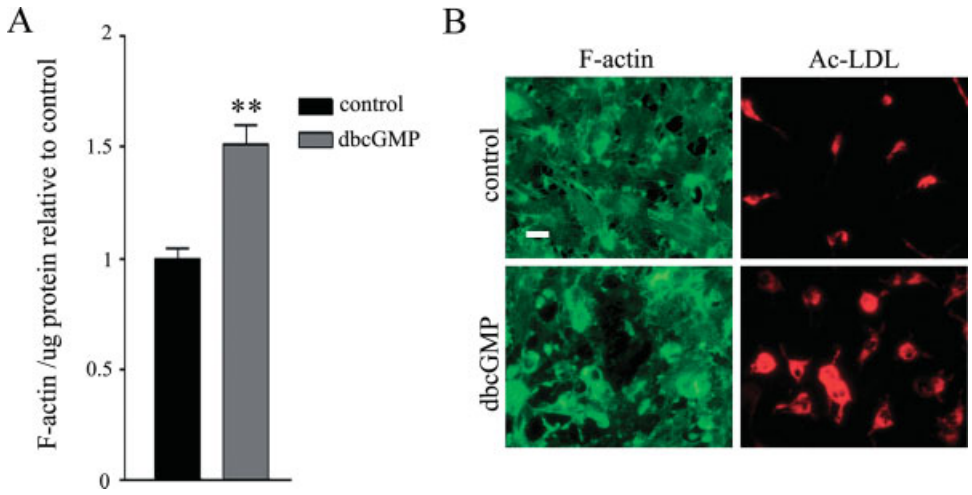

Fig. 1. Effect of dbcGMP on F-actin content and microglial morphology in cerebellar astrocyte-enriched cultures. Confluent (14 DIV) rat cerebellum astrocyte-enriched cultures were exposed for 18–24 h to vehicle (control, black bars) or dbcGMP (100 μM, gray bars). (**A**) F-actin quantification. Fluorescence of rhodamine–phalloidin bound to F-actin was measured as indicated in Methods. Results in fluorescence units/μg protein are presented relative to control and are means ± SEM of four different experiments. **Statistically significant difference versus control ($P < 0.01$) evaluated by Student's t test. (**B**) Double-staining for F-actin (green) and the microglial marker Dil-Ac-LDL (red). Note the change in morphology and intense F-actin staining in Dil-Ac-LDL-positive cells in cultures treated with dbcGMP. Scale bar, 20 μm. [Color figure can be viewed in the online issue, which is available at www.interscience.wiley.com.]

Measurement of Nitrites

Nitrite accumulation was assayed in the culture media by the Greiss reaction as previously described in Baltrons and Garcia (1999).

Statistical Analysis

Quantifiable determinations were expressed as mean ± standard error (SEM) of the indicated number of experiments performed in different culture preparations. Data analysis was carried out using Graph Pad Prism Software (Version 4). When comparing more than two groups, significance of differences was evaluated by one-way ANOVA followed by Turkey's *post hoc* test or two-way ANOVA followed by Bonferroni's *post hoc* test. For comparison of two groups the Student's t test was used. Results expressed as ratios were subjected to arcsine transformation before statistical analysis to ensure a normally distributed data set.

RESULTS

DbcGMP Induces a Morphological Change and Increases F-Actin in Microglia Present in Astrocyte-Enriched Cultures

We recently reported that the cGMP-PKG pathway induces a profound reorganization of the actin cytoskeleton in cultured astrocytes (Boran and Garcia, 2007). In the course of those studies, we observed that treatment of rat cerebellar astrocyte-enriched cultures (14 DIV) with the cGMP analog dbcGMP (100 μM, 24 h), produced a significant increase in the content of F-actin (Fig. 1A). We have previously shown that in these cultures, microglia can comprise up to 20–30% of total cells (Agullo et al., 1995). Double-staining of cultures for F-actin and the microglial marker Dil-Ac-LDL (Fig. 1B), showed that the dbcGMP treatment provoked a drastic change in the morphology of microglia from the elongated and ramified shape these cells show in contact with astrocytes to a round enlarged ameboid-type morphology typical of activated microglia. Additionally, these enlarged microglial cells showed strong F-actin staining indicating that the increase in F-actin content in the astrocyte-enriched cultures occurs in contaminating microglia.

The NO-cGMP Pathway Is Not Involved in LPS-Induced Reorganization of F-Actin in Microglia

In our previous study, we showed that the reorganization of F-actin induced by LPS in cultured astrocytes occurred to a large extent via the NO-cGMP-PKG pathway (Boran and Garcia, 2007). Additionally, we observed that similar to dbcGMP, LPS increased F-actin content in astrocyte-enriched cultures. We thus investigated if the LPS-induced increase in F-actin was taking place in microglia and if it involved the NO-cGMP pathway. As shown in Fig. 2A, the LPS effect occurred in microglia because it could not be observed in cultures treated with cytosine arabinoside (Cyt-ara, 10 μM from 10 to 14 DIV), a condition we previously demonstrated (Agullo et al., 1995) and also show here (Fig. 2B) to be highly effective in decreasing microglial contamination. Double-staining of astrocyte-enriched cultures for F-actin and Dil-Ac-LDL showed that LPS (18–24 h, 100 ng/mL) induced a similar change in morphology and F-actin staining in contaminating microglia as that observed with dbcGMP treatment (Fig. 2B). However, the LPS-induced increase in F-actin was not prevented by the NO-sensitive guanylyl cyclase (GC_{NO}) inhibitor ODQ (20 μM; Fig. 2A) indicat-

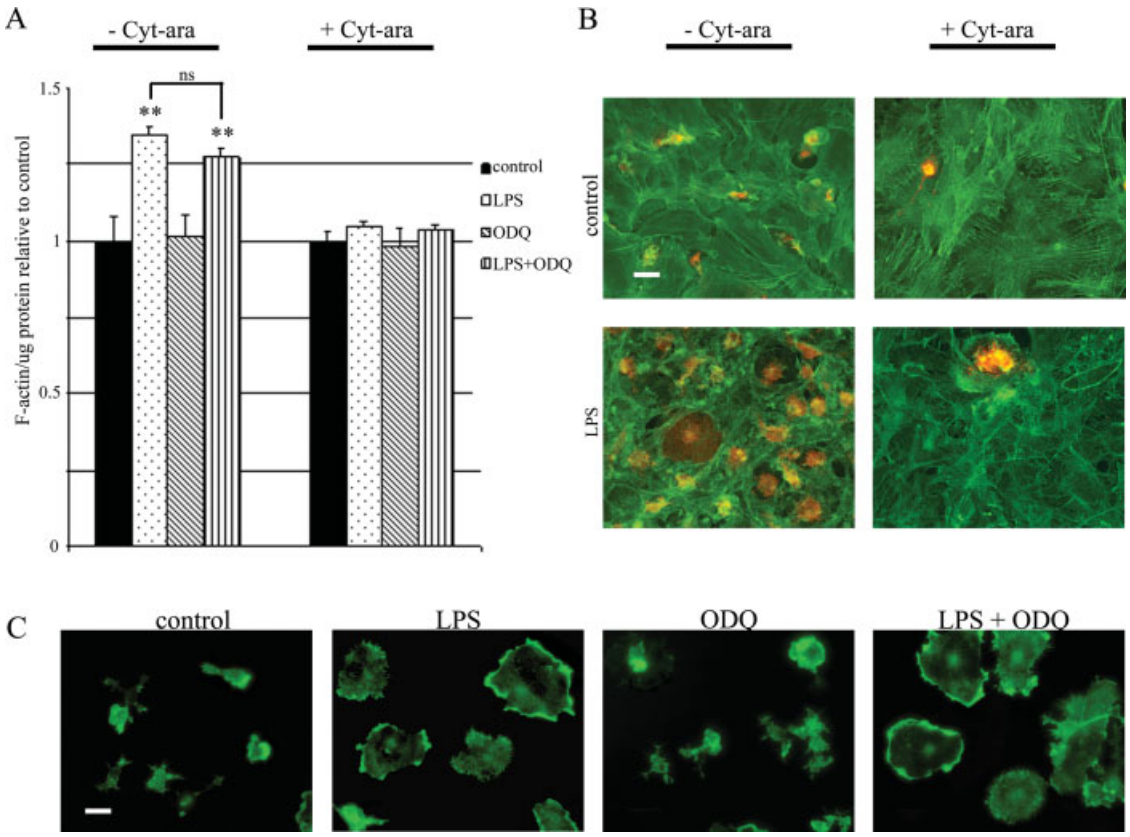

Fig. 2. Effect of LPS on F-actin content and distribution in glial cultures. Astrocyte-enriched cultures treated or not with Cyt-ara (10 μM) to decrease microglial contamination (**A** and **B**) or pure microglial cultures (**C**) were exposed for 18–24 h to LPS (100 ng/mL), ODQ (20 μM) or both. (A) Results from F-actin quantification in fluorescence units per microgram protein are presented relative to controls and are means ± SEM of four different experiments. **Statistically significant difference versus respective controls ($P < 0.01$) evaluated by one-way ANOVA followed by Turkey's *post hoc* test; ns, not significant. (B) Double-staining for F-actin (green) and the microglial marker Dil-Ac-LDL (red). Note the change in morphology and intense F-actin staining in Dil-Ac-LDL-positive cells in cultures treated with LPS. (C) F-actin staining in pure microglial cultures. Note that ODQ does not prevent the change in morphology induced by LPS. Scale bars, 20 μm.

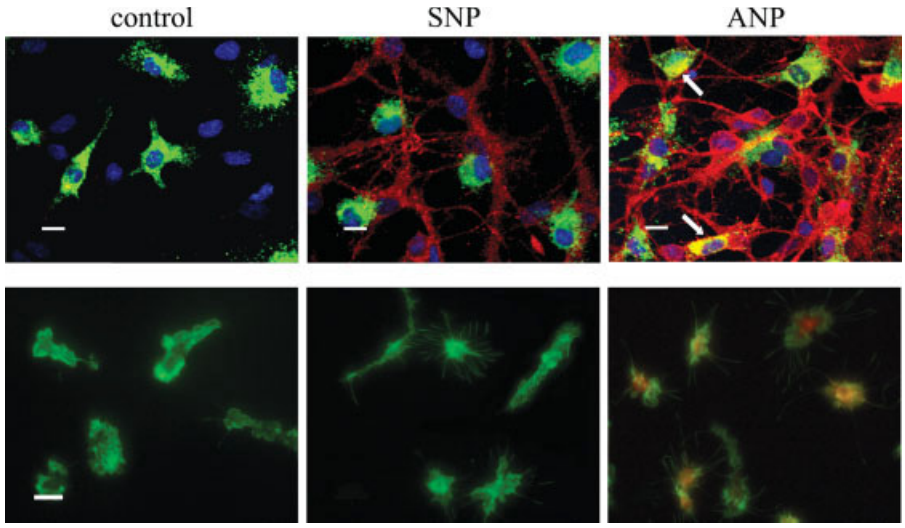

Fig. 3. Stimulation of cGMP formation by ANP but not by a NO donor in microglia. Astrocyte-enriched cultures and pure microglial cultures were treated for 3 min at 37°C with vehicle (control), SNP (100 μM), or ANP (1 μM) in the presence of IBMX (1 mM). Top row: Astrocyte-enriched cultures stained for contaminating microglia (Alexa 488-Ac-LDL, green), nuclei (DAPI, blue), and cGMP (anti-cGMP antibody, red) and observed by confocal microscopy. Scale bars, 10 μm. Arrows point to Alexa 488-Ac-LDL- and cGMP- positive cells. Bottom row: Microglial cultures double-stained for F-actin (green) and cGMP (red). Scale bar, 20 μm. Note that cGMP immunostaining is increased in astrocytes in response to both SNP and ANP but only in response to ANP in microglia.

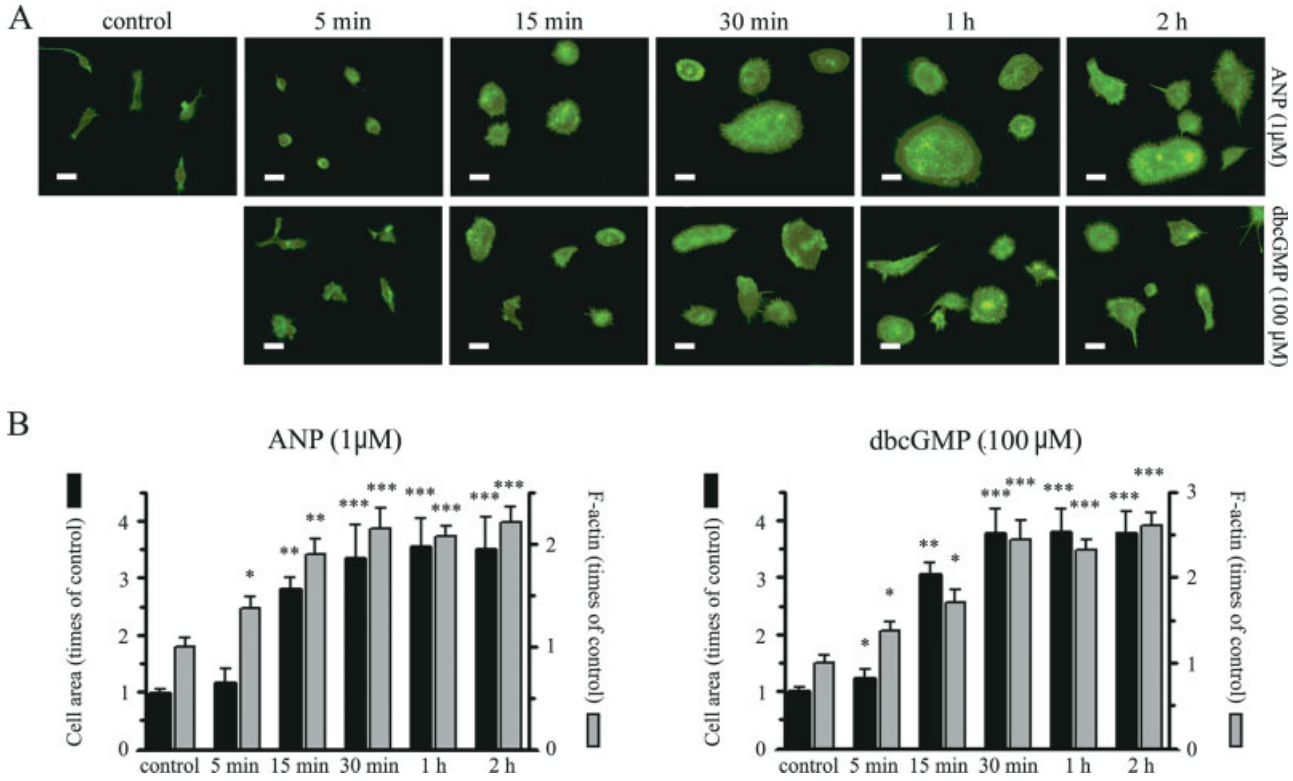

Fig. 4. Time course of the morphological changes and F-actin redistribution induced by ANP and dbcGMP in microglial cells. (**A**) Microglial cultures were left untreated (control) or treated with 1 μM ANP (top row) or 100 μM dbcGMP (bottom row) for the indicated times and stained for F-actin. Scale bars, 20 μm. (**B**) Quantification of microglial cell area (black bars) and F-actin fluorescence intensity (gray bars) for ANP-treated (B left) and dbcGMP-treated (B right) cells determined by using MetaMorph Software (Version 6.1). Results are expressed relative to each control value and are means ± SEM of 100 cells counted per assayed time in each of three independent experiments. Statistically significant differences versus respective controls evaluated by one-way ANOVA followed by Turkey's *post hoc* test: $^{*}P < 0.05$; $^{**}P < 0.01$; $^{***}P < 0.001$. [Color figure can be viewed in the online issue, which is available at www.interscience.wiley.com.]

ing that it is independent of the NO-cGMP pathway. Furthermore, using pure microglial cultures prepared from astrocyte-enriched cultures by mild trypsinization (see Materials and Methods) we showed that the morphological change induced by LPS in microglia was also independent of GC_{NO} activity (Fig. 2C).

cGMP is Formed in Microglial Cells in Response to NPs but Not to NO Donors

The ability of dbcGMP to reorganize the microglial F-actin cytoskeleton together with the lack of involvement of the NO-cGMP pathway in the effects of LPS prompted us to investigate if microglial cells were able to generate cGMP endogenously. For that purpose, astrocyte-enriched cultures were stimulated for 3 min with the NO-donor SNP (100 μM) or with ANP (1 μM) in the presence of the phospholiesterase inhibitor IBMX (1 mM). Cells were double-stained for the microglial marker Alexa 488-Ac-LDL and for cGMP and then examined by confocal microscopy. As expected, both NO and ANP were able to stimulate cGMP formation in astrocytes. However, Alexa 488-Ac-LDL-positive cells were immunostained with the anti-cGMP antibody only after stimulation with ANP (Fig. 3, top row). The same results were observed in pure microglial cultures (Fig. 3, bottom row). cGMP immunostaining was also detected in microglial cells after treatment with CNP (3 min, 1 μM), although with less intensity than with ANP (data not shown). In the microglial cultures, no significant cGMP immunostaining was observed after exposure for longer times (up to 120 min) to SNP or the NO-independent activator of the GC_{NO} BAY 41-2272 (10 μM) in the presence of IBMX (Supplementary Fig. 2). Thus, rat brain microglia appears to express a functional particulate GC (pGC) but no GC_{NO} activity whether co-cultured with astrocytes or in pure cultures.

ANP and dbcGMP Induce a Rapid and Concentration-Dependent Change in Cell Shape and Actin Cytoskeleton in Microglia Via PKG

To provide further evidence on the involvement of cGMP in regulating microglia cell shape and cytoskeleton dynamics, we investigated the effects of ANP and dbcGMP as a function of time and concentration in pure microglial cultures. As shown in Fig. 4A in cells stained for F-actin, the morphological change induced by ANP (1 μM, up) and dbcGMP (100 μM, bottom) results from a profound reorganization of the F-actin cytoskeleton that is evident at the shortest time studied (5 min). Microglia loses the ramified appearance and transforms into round

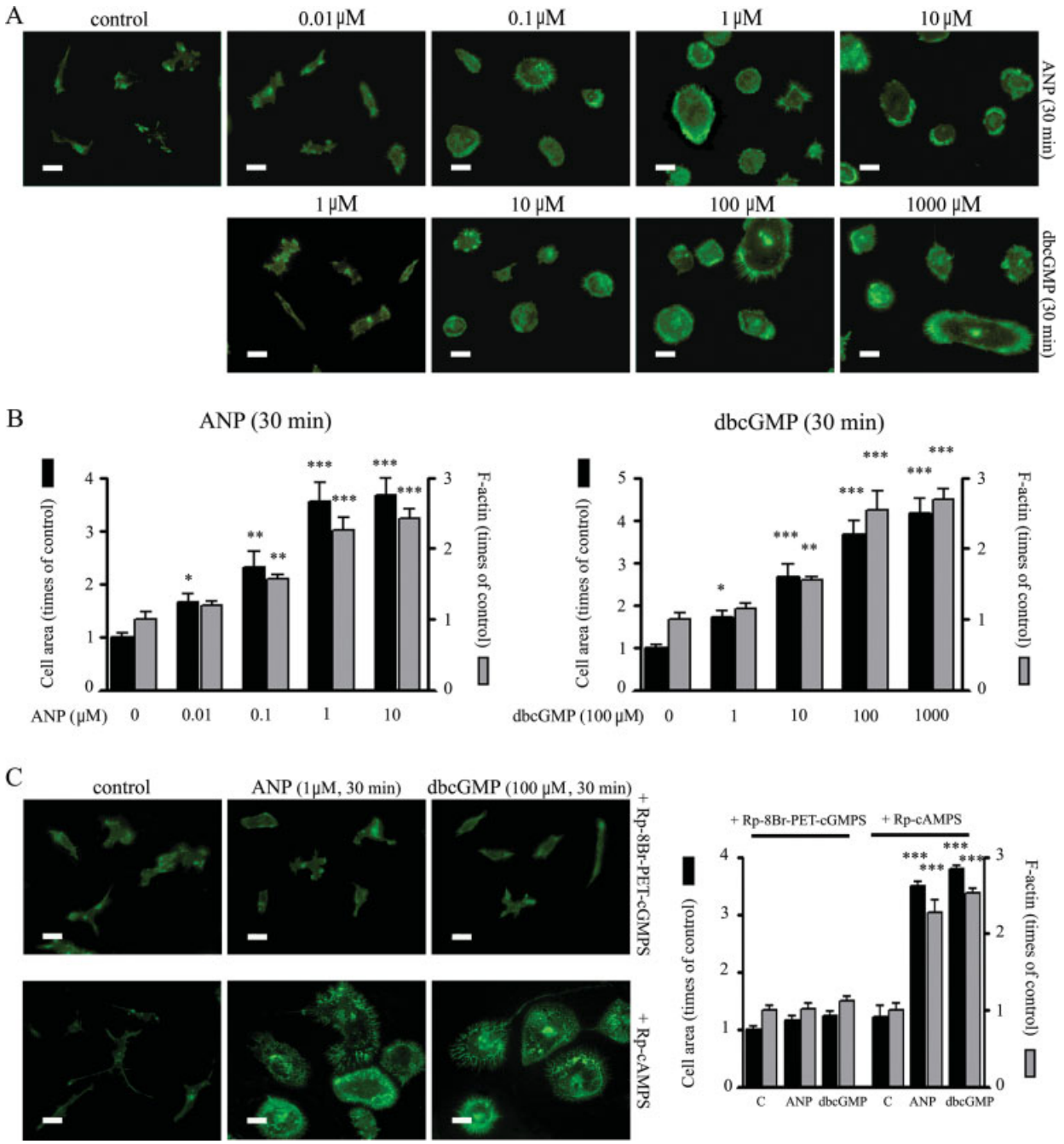

Fig. 5. Concentration-dependence of the effect of ANP and dbcGMP on morphological changes and F-actin redistribution in microglial cells. Implication of PKG activity. (**A**) Microglial cultures were left untreated (control) or treated for 30 min with ANP (top row) or dbcGMP (bottom row) at the indicated concentrations and stained for F-actin. (**B**) Quantification of microglial cell area (black bars) and F-actin fluorescence intensity (gray bars) for ANP-treated (B left) and dbcGMP-treated (B right) cells. Results are expressed relative to each control value and are means ± SEM of 100 cells counted per assayed concentration in each of three independent experiments. Statistically significant differences versus respective controls evaluated by one-way ANOVA followed by Turkey's *post hoc* test: $^{*}P < 0.05$; $^{**}P < 0.01$; $^{***}P < 0.001$. (**C**) Cells were pretreated for 1 h with Rp-8Br-PET-cGMPS (0.5 μM, up) or with Rp-cAMPS (150 μM, bottom) and then exposed for 30 min to vehicle (control), ANP 1 μM or dbcGMP 100 μM. Cells were then stained for F-actin (green) and cell area and fluorescence intensity quantified as in B. Scale bars, 20 μm. [Color figure can be viewed in the online issue, which is available at www.interscience.wiley.com.]

and bigger cells that show intense accumulations of F-actin staining in certain areas of the soma. F-actin staining is also observed decorating lamellipodia and filopodia. For both compounds, the maximum change in microglia size and F-actin labeling was observed after 30 min of treatment (Fig. 4B) and was still observed after 24 h. At 30 min, significant effects could be detected at concentrations as low as 0.01 μM ANP and 1 μM dbcGMP (Fig. 5A) and maximal effects were observed at 1 and 100 μM, respectively (Fig. 5B). These effects were

totally prevented by pretreatment (1 h) with the specific PKG inhibitor Rp-8Br-PET-cGMPS (0.5 μM) whereas they were unaltered by preincubation with the specific PKA inhibitor Rp-cAMPS (150 μM); (Fig. 5C).

Rho GTPases Are Involved in cGMP-Induced Morphological Changes in Microglia

The Rho GTPase family of small G proteins (RhoA, Rac, and Cdc42) controls the organization and dynamics of the actin cytoskeleton in all eukaryotic cells (Etienne-Manneville and Hall, 2002; Hall, 1998). Activation of RhoA causes cell contraction, whereas activation of Rac promotes formation of lamellipodial extensions and membrane ruffles, and activation of Cdc42 triggers the development of filopodia (Mackay and Hall, 1998). Since cGMP-mediated pathways have been implicated in the regulation of activity and expression of Rho GTPases in different cell types (Boran and Garcia, 2007; Gudi et al., 2002; Krepinsky et al., 2003; Sandu et al., 2001; Sauzeau et al., 2000, 2003; Sawada et al., 2001), we investigated if regulation of Rho GTPase activity was involved in cGMP effects in microglia. As shown in Fig. 6, the Rho GTPase activator geranylgeranyl-pyrophosphate (GGpp) prevents ANP-induced morphological changes in microglia in a concentration-dependent manner (Fig. 6A) suggesting that inhibition of at least one of the Rho GTPases is involved in the ANP effect. In contrast, Y-27632 (20 μM) an inhibitor of the RhoA target kinase ROCK, mimics the effect of ANP in cell rounding but does not induce lamellipodia and filopodia formation (Fig. 6B). However, addition of increasing concentrations of ANP (2 h) to Y-27632 treated-cells (10 min) caused a concomitant increment in lamellipodia and filopodia formation (Fig. 6B) suggesting that Rac and Cdc42 activation must also occur as a consequence of the stimulation of the cGMP-PKG pathway. To confirm that inhibition of RhoA and activation of Rac and Cdc42 were involved in cGMP-induced changes in the microglial actin cytoskeleton, we transfected cells with a constitutively active RhoA mutant (V14RhoA) or with dominant negative Rac1 or Cdc42 mutants (N17Rac1 and N17Cdc42, respectively). Transfected cells were visualized by anti-myc or anti-FLAG and double-labeled for F-actin. Cells transfected with empty vectors (pEXV3 and pCMV) presented the same morphology as nontransfected both in controls and in ANP-treated cells, ruling out transfection artefacts (Supplementary Fig. 3). Round-shaped cells and cells presenting lamellipodia/membrane ruffles or filopodia were counted in transfected and untransfected cells in the same dishes. As shown in Fig. 6C, cells transfected with mutants V14RhoA, N17Rac1, or N17Cdc42 and treated with ANP neither did acquire a round-shape nor presented lamellipodia or filopodia, respectively (see representative cells indicated by arrows a, b, and c). In contrast, nontransfected cells in the same dishes presented a similar actin cytoskeletal reorganization in response to ANP as that described earlier (see representative cells indicated by arrows d, e, and f).

The cGMP/PKG Pathway Stimulates Microglia Phagocytic Activity. Implication of Rho GTPases

Since cGMP-induced alterations in microglial actin cytoskeleton resemble those described in reactive gliosis (Bohatschek et al., 2001; Raivich et al., 1999; Streit and Kreutzberg, 1988), we analyzed if the cGMP-PKG pathway was also involved in the regulation of the microglial phagocytic response. Primary microglial cultures were treated with tetramethylrhodamine-conjugated *E. coli* particles (0.1 mg/mL) in the presence or absence of ANP (1 μM) or dbcGMP (100 μM) for 30 min at 37°C, fixed and stained for F-actin (Fig. 7A). Increases of 3-fold in the number of *E. coli* particles/cell were quantified for both ANP and dbcGMP treatments (Fig. 7B, up). Pretreatment with the PKG inhibitor Rp-8Br-PET-cGMPS (0.5 μM, added 1 h before) prevented ANP and dbcGMP effects indicating that PKG activation is involved in cGMP-stimulated microglia phagocytic activity. Similar results were obtained when red fluorescence inert particles instead of *E. coli* particles were used (Fig. 7B, bottom), indicating that microglia activation by bacterial molecules is not required for induction of the phagocytic response by cGMP.

Since inhibition of RhoA-ROCK and activation of Rac and Cdc42 is involved in the actin reorganization and morphological change induced by cGMP in microglia, we investigated the implication of these Rho GTPase family members in the cGMP phagocytic response. As shown in Fig. 7C, when microglial cultures were incubated with inert particles in the presence of the Rho GTPase activator GGpp (10 μM, 30 min) no significant engulfment of particles was observed and, furthermore, GGpp prevented ANP-induced phagocytosis. In contrast, the ROCK inhibitor Y-27632 (20 μM, 30 min) was able to elicit a more than 2-fold increase in the number of internalized particles/cell, but co-incubation with ANP (1 μM) further increased the phagocytic response to fourfold indicating that inhibition of ROCK is not sufficient to explain the ANP effect. In agreement with this, co-incubation with Y-27632 and GGpp elicited a phagocytic response of the same magnitude as ANP suggesting that both inhibition of RhoA-ROCK and activation of Rac and/or Cdc42 are involved in the ANP response. To confirm this, we examined the phagocytic activity of cells transfected with V14RhoA, N17Rac1, and N17Cdc42 mutants. As shown in Fig. 7D, microglia overexpressing constitutively active RhoA was not able to engulf inert particles whether stimulated or not with ANP indicating that inhibition of the RhoA-ROCK pathway is a necessary event for ANP-induced phagocytosis. In addition, overexpression of dominant negative Rac1 or Cdc42 reduced the ANP effect by 68 and 52%, indicating that both Rac1 and Cdc42 play a role in the mechanism of ANP-induced phagocytosis in microglia. The implication of Rac1 and Cdc42 and the dominant negative role of RhoA in ANP-induced phagocytosis suggests a mechanism similar to that described for apoptotic cell phagocytosis (Leverrier and Ridley, 2001; Tosello-Trampont et al., 2003).

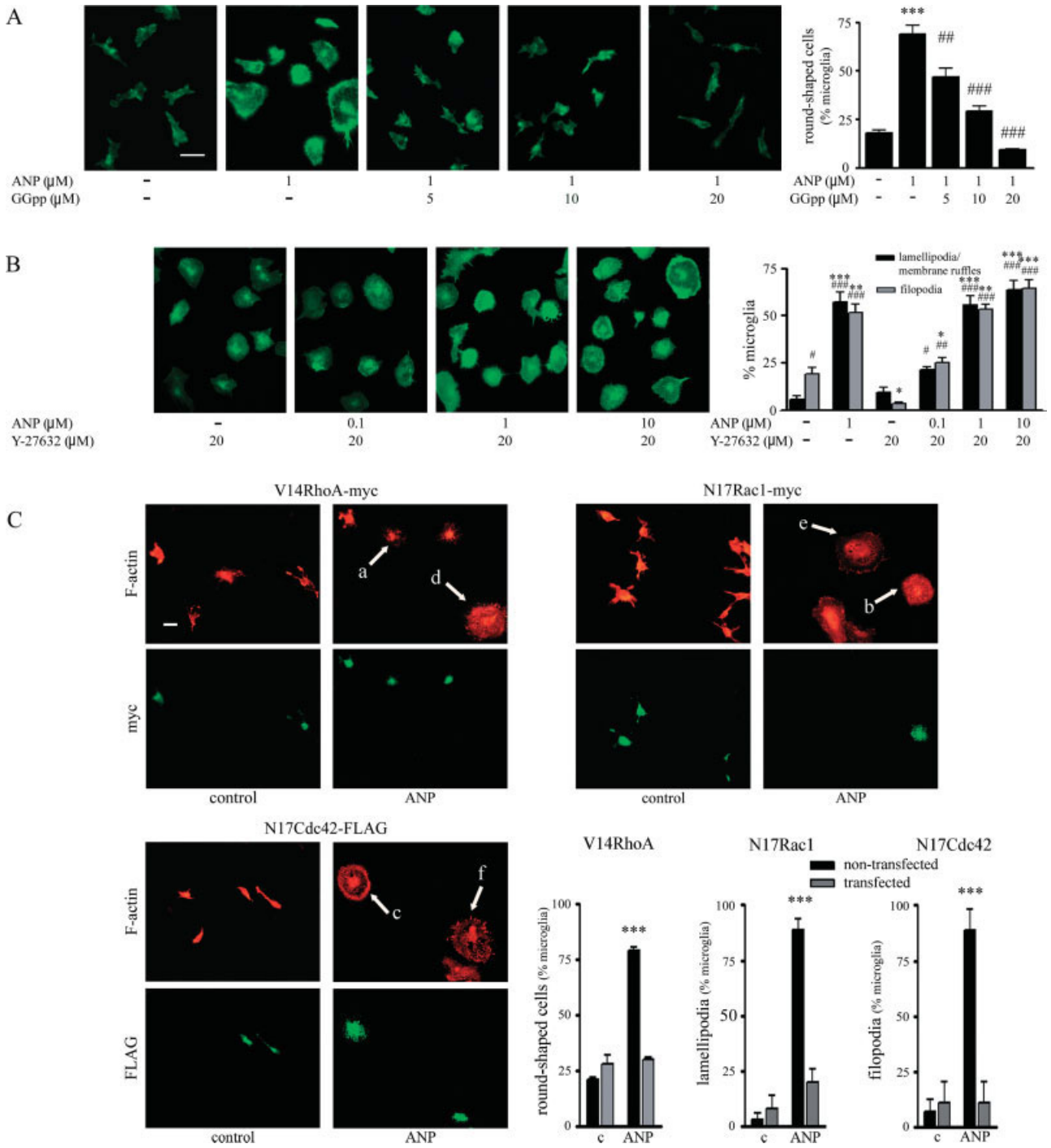

Fig. 6. Implication of Rho-GTPases in the actin cytoskeleton reorganization induced by ANP in microglial cells. (**A**) Microglial cultures were pretreated with increasing concentrations of geranylgeranyl pyrophosphate (GGpp) for 10 min before adding ANP (1 μM) for 2 h and cells were stained for F-actin. Scale bar, 20 μm. Round-shaped cells were quantified for each treatment and values are presented as means ± SEM per cent of 100 cells analyzed in four independent experiments. A cell was consider to be round when the ratio between its minor and maximal radio length is higher than 0.6, evaluated by using MetaMorph Software (Version 6.1). ** and $^{\#\#}P < 0.01$; *** and $^{\#\#\#}P < 0.001$ are statistically significant differences versus respective controls and ANP treatment, respectively, evaluated by Turkey's *post hoc* test after one-way ANOVA. (**B**) Microglial cultures were pretreated with the ROCK inhibitor Y-27632 (20 μM) for 10 min, and treated with increasing concentrations of ANP for 2 h. Afterwards, cells were stained for F-actin. Cells containing lamellipodia/ membrane ruffles (black bars) and filopodia (gray bars) were counted and analyzed as in A. A cell was consider to have lamellipodia or membrane ruffles when they are visible at ×20 objective magnification and to contain filopodia when at least 10 filaments around the cell surface can be counted at this magnification * and $^{\#}P < 0.05$; ** and $^{\#\#}P < 0.01$; *** and $^{\#\#\#}P < 0.001$ are statistically significant differences versus controls and Y-27632 treatment, respectively. (**C**) Cultures were transfected with expression vectors containing the following mutants: a constitutively active RhoA, V14RhoA, or the negative dominants for Rac1 and Cdc42, N17Rac1 or Cdc42, respectively. After treating with vehicle (control) or ANP 1 μM for 2 h, cells were double-stained for F-actin (red) and myc (for RhoA and Rac1 detection) or FLAG (for Cdc42) (green). Scale bars, 50 μm. Arrows a, b, and c indicate transfected cells treated with ANP that do not present round-shape, lamellipodia and filopodia, respectively. Arrows d, e, and f indicate nontransfected cells that show the morphological change described for ANP treatment. Round-shaped cells, cells presenting lamellipodia/membrane ruffles or filopodia were counted for untransfected cells and cells transfected with pEXV3-V14RhoA-myc, pEXV3-N17Rac1-myc, and pCMV-N14Cdc42-FLAG, respectively. Values are expressed as a percentage of total microglia and are means ± SEM of at least 75 cells counted for each condition in three independent experiments. $^{***}P < 0.001$: significant difference versus control calculated by two-way ANOVA followed by Bonferroni's *post hoc* test. [Color figure can be viewed in the online issue, which is available at www.interscience.wiley.com.]

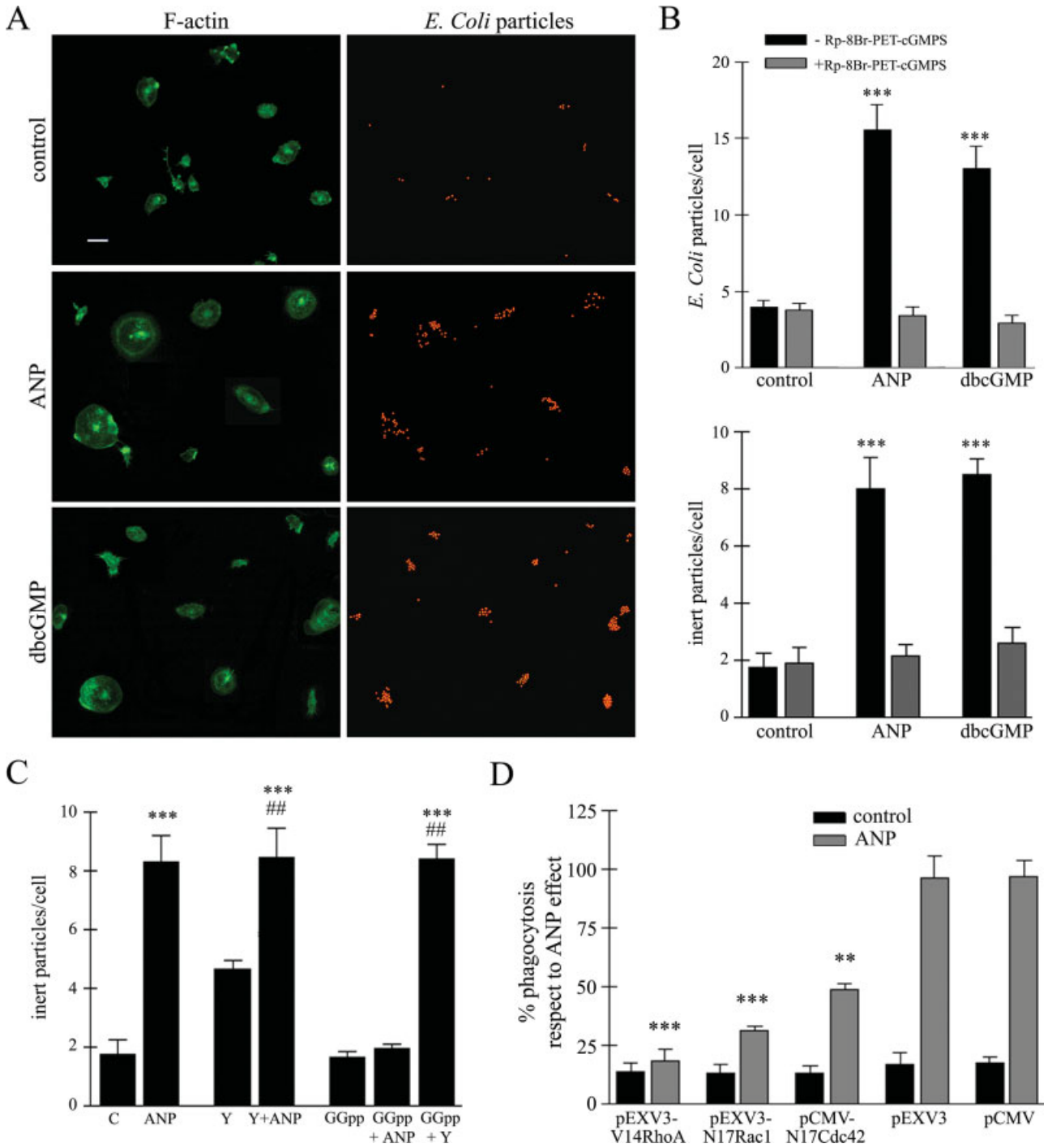

Fig. 7. Effect of ANP and dbcGMP on the phagocytic activity of microglial cells. Microglial cultures were treated with tetramethylrhodamine-conjugated *E. coli* particles or inert particles (0.1 mg/mL, red) and vehicle (control), ANP (1 μM) or dbGMP (100 μM) for 30 min at 37°C. Then cells were fixed and stained for F-actin (green). (**A**) Fluorescence images of cells treated with *E. coli* particles. Scale bar, 30 μm. (**B**) Quantification of *E. coli* particles (up) and inert particles (bottom) in microglial cells stained as in A. Cultures were pretreated (gray bars) or not (black bars) for 1 h with Rp-8Br-PET-cGMPS (0.5 μM). Results are expressed as particles/cell and they are means ± SEM of three independent experiments in which at least 100 cells per treatment were counted in each experiment. Statistically significant differences respects to controls were evaluated by two-way ANOVA followed by Bonferroni's *post hoc* test: $^{***}P < 0.001$. (**C**) Microglial cultures were treated with ANP (1 μM), Y-27632 (Y, 20 μM), GGpp (10 μM), or the indicated combinations together with fluorescent inert particles for 30 min at 37°C and then cells were stained as above. $^{**}P < 0.01$; $^{***}P < 0.001$ are differences respect to control and $^{\#\#}P < 0.01$ is difference respect to Y-27632-treated cultures calculated by Turkey's *post hoc* test prior to one-way ANOVA. (**D**) Cultures transfected with expression vectors containing a constitutively active RhoA (pEXV3-V14RhoA) or the negative dominants for Rac1 and Cdc42 (pEXV3-N17Rac1 or pCMV-Cdc42, respectively) and treated with inert particles and vehicle (control, black bars) or ANP (gray bars, 1 μM) for 30 min. Transfections with empty vectors were also assayed (pEXV3 and pCMV). Values are expressed as a percentage of particles/cell in nontransfected cells in the same dishes treated by ANP for each construct transfection and they are means ± SEM of at least 50 transfected cells counted for each condition in three different assays. $^{**}P < 0.01$; $^{***}P < 0.001$: significant differences versus respective empty vector calculated by two-way ANOVA followed by Bonferroni's *post hoc* test. [Color figure can be viewed in the online issue, which is available at www.interscience.wiley.com.]

ANP Decreases LPS-Induced NOS-2 and TNF-α Expression in Microglia

In macrophages, FcγR-mediated phagocytosis is accompanied by release of proinflammatory mediators, while complement-mediated phagocytosis does not initiate a proinflammatory response, and apoptotic cell ingestion is anti-inflammatory (Aderem and Underhill, 1999; Erwig and Henson, 2007). Thus, we investigated if the phagocytic phenotype induced by stimulation of the ANP-cGMP-PKG pathway in microglia was associated with increased expression of the typical proinflammatory genes NOS-2 and TNF-α. As shown in Figs. 8 and 9, treatment of astrocyte-enriched cultures or pure microglial cultures for 24 h with a concentration of ANP (1 μM) maximally effective in inducing actin cytoskeleton rearrangements was not able to increase NOS-2 protein levels or activity (nitrite accumulation) in microglial or astroglial cells. However, when cells were challenged with LPS (100 ng/mL, 24 h) a large increase in NOS-2 protein and activity was observed in both types of cultures as expected. Double-immunofluorescence staining with anti-NOS-2 and the microglial marker CD68 demonstrated that in astrocyte-enriched cultures NOS-2 induction in response to LPS is more prominent in contaminating microglia (Fig. 8A), in agreement with previous reports (Galea et al., 1992; Sola et al., 2002). Co-treatment with ANP (1 μM) significantly reduced the intensity of NOS-2 immunofluorescence, protein levels, and nitrite accumulation (Figs. 8A–D). In pure microglial cultures, all cells presented increased NOS-2 immunoreactivity when treated with LPS (Fig. 9A) and ANP similarly reduced NOS-2 staining and nitrite accumulation (Figs. 9A,B). Preincubation of these cultures with Rp-8Br-PET-cGMPS (0.5 μM) prevented the decrease in nitrite accumulation (Fig. 9B) indicating that decrease of LPS-induced NOS-2 expression by ANP also requires PKG activity.

Analysis of TNF-α immunostaining in astrocyte-enriched cultures showed that LPS increased TNF-α in microglia as well as in astrocytes, whereas ANP alone had no effect on either cell type (Fig. 8E). However, when LPS was co-incubated with ANP, TNF-α immunostaining was significantly decreased (Fig. 8E). An equal pattern was observed when TNF-α released to the media was analyzed by flow cytometry (Fig. 8F). Similar results were obtained in pure microglial cultures (Figs. 9C,D).

cGMP Induces Amoeboid Morphology and Increased CD11b Expression but Decreases NOS-2 Induction in Hippocampal Organotypic Cultures

To verify if the cGMP effects observed in cultured microglia also take place in a setting closer to the *in vivo* brain structure, we examined the effect of ANP (1 μM, 24 h) or dbcGMP (100 μM, 24 h) in 400-μm slices from rat hippocampus maintained in culture for 10–12 days as described in Materials and Methods. As previously reported (Abraham et al., 2001), under these culture conditions microglia, labeled with the specific marker CD11b, presented a ramified morphology typical of resting microglia and did not express NOS-2 (Fig. 10A). However, when slices were treated with ANP or dbcGMP, CD11b-positive cells acquired an amoeboid morphology and showed a significant increase in CD11b immunofluorescence (Figs. 10A,B). Treatment of the slices with LPS (1 μg/mL, 24 h) produced a similar cell shape change and increase in CD11b immunofluorescence. Additionally, in agreement with results in cell cultures LPS increased NOS-2 imunofluorescence in CD11b-positive cells, whereas ANP and dbcGMP did not and both these compounds were able to inhibit the LPS effect to a large extent (Figs. 10A,B).

DISCUSSION

In this study, we demonstrate for the first time that stimulation of the cGMP-PKG axis by ANP in rat brain microglial cells induces profound actin cytoskeleton rearrangements promoting an increase in size, rounding, and formation of lamellipodia and filopodia in the cell periphery. We initially observed cGMP-induced F-actin increases and morphological changes in the microglia present in astrocyte-enriched cultures where the majority of these cells show a ramified morphology reminiscent of that of resting microglia in normal brain (Agullo et al., 1995; Kalla et al., 2003). We confirmed these observations in primary microglial cultures as well as in hippocampal organotypic cultures stimulated with ANP or the cGMP analog dbcGMP. The actin cytoskeleton alterations induced by these compounds in microglia are similar to those induced by LPS in this and other studies (abd-el-Basset and Fedoroff, 1995; Kloss et al., 2001). However, in contrast to our recent report showing NO-cGMP-mediated effects of LPS in the astroglial actin cytoskeleton (Boran and Garcia, 2007), the increase in F-actin or the rounding and enlargement of the microglial cells induced by LPS do not seem to be mediated by the NO-cGMP pathway since they are not prevented by the GC_{NO} inhibitor ODQ. This was not surprising since we had previously observed that rat brain microglia in culture did not accumulate cGMP in response to NO donors indicating that these cells do not express an active GC_{NO} (Agullo et al., 1995). We confirm this observation here by cGMP immunocytochemistry in microglia in isolated culture as well as co-cultured with astrocytes. In contrast, we observed increased cGMP immunoreactivity in microglia when the stimuli were ANP or CNP. Similar observations were reported in cells labeled with a microglial marker in spheroid cultures from rat brain (Teunissen et al., 2000). In accordance, expression of mRNAs for ANP receptors (Types A, B, and C) has been recently demonstrated in rat microglial cultures (Moriyama et al., 2006). In contrast to our results, inhibitors of GC_{NO} have been reported to prevent LPS induction of the activated microglia marker CD11b in the mouse microglial cell line BV2 (Roy et al., 2006), suggesting differences in GC_{NO} expression in rat versus mouse microglia or in

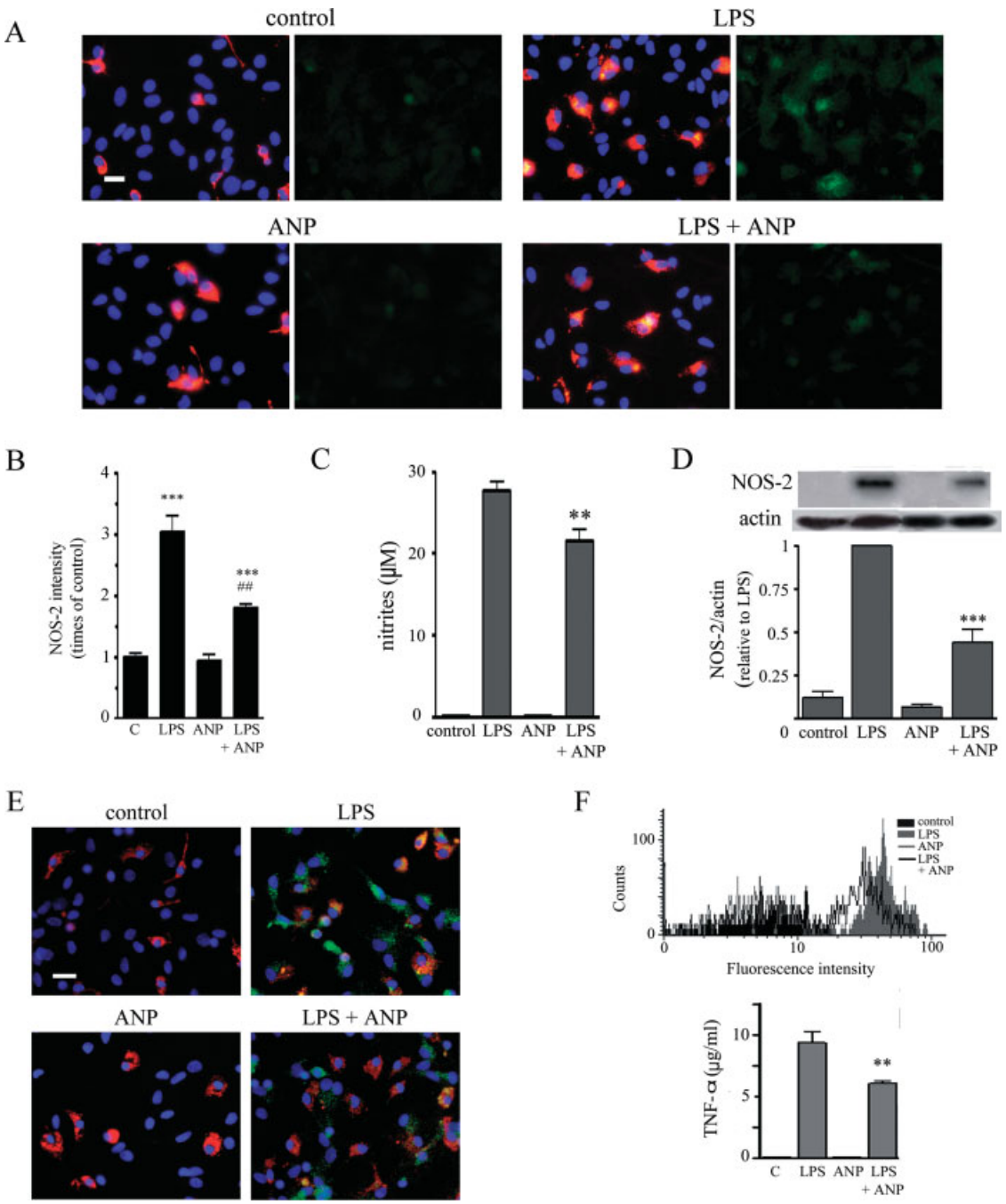

Fig. 8. Effect of ANP on LPS-induced NOS-2 and TNF-α in astrocyte-enriched cultures. (**A**) Cultures untreated (control) or treated with LPS (100 ng/mL), ANP (1 μM) or both for 24 h, were fixed and stained for CD68 (red), NOS-2 (green) and DAPI (blue). Scale bar, 20 μm. Note that CD68-positive cells (microglia) stain more intensely for NOS-2 than CD68-negative cells (astrocytes). (**B**) NOS-2 fluorescence intensity was quantified in microglial cells by using MetaMorph Software (Version 6.1) and is expressed relative to controls. Results are means ± SEM of four different experiments analyzing at least 200 cells per treatment in each experiment. Significant difference versus control: $^{***}P < 0.001$ and versus LPS treatment: $^{\#\#\#}P < 0.001$. (**C**) Nitrite accumulation was determined in the incubation media after 48 h in cultures treated as in A. Results are means ± SEM of three different experiments. Significant difference versus LPS treatment $^{**}P < 0.01$. (**D**) Western blot of NOS-2 in cultures treated as in A. Actin was used as control for the amount of protein loaded (top). Densitometric quantification of NOS-2/actin in the immunoblots (bottom). Values are expressed relative to LPS treatment and represent means ± SEM of five different cultures. Significant difference versus LPS treatment $^{***}P < 0.001$. (**E**) Staining for TNF-α (green), CD68 (red) and DAPI (blue) in cultures treated as in A. Scale bar, 25 μm. Note TNF-α staining in CD68 positive (microglia) and negative (astrocytes) cells in LPS-treated cultures. (**F**) Representative cytometric analysis of TNF-α levels determined in the incubation media after 24 h in cultures treated as in A (up). Quantification shows means ± SEM of three different experiments (bottom). Significant difference versus LPS treatment: $^{**}P < 0.01$. Statistically significant differences were evaluated by one-way ANOVA followed by Turkey's *post hoc* test in all cases.

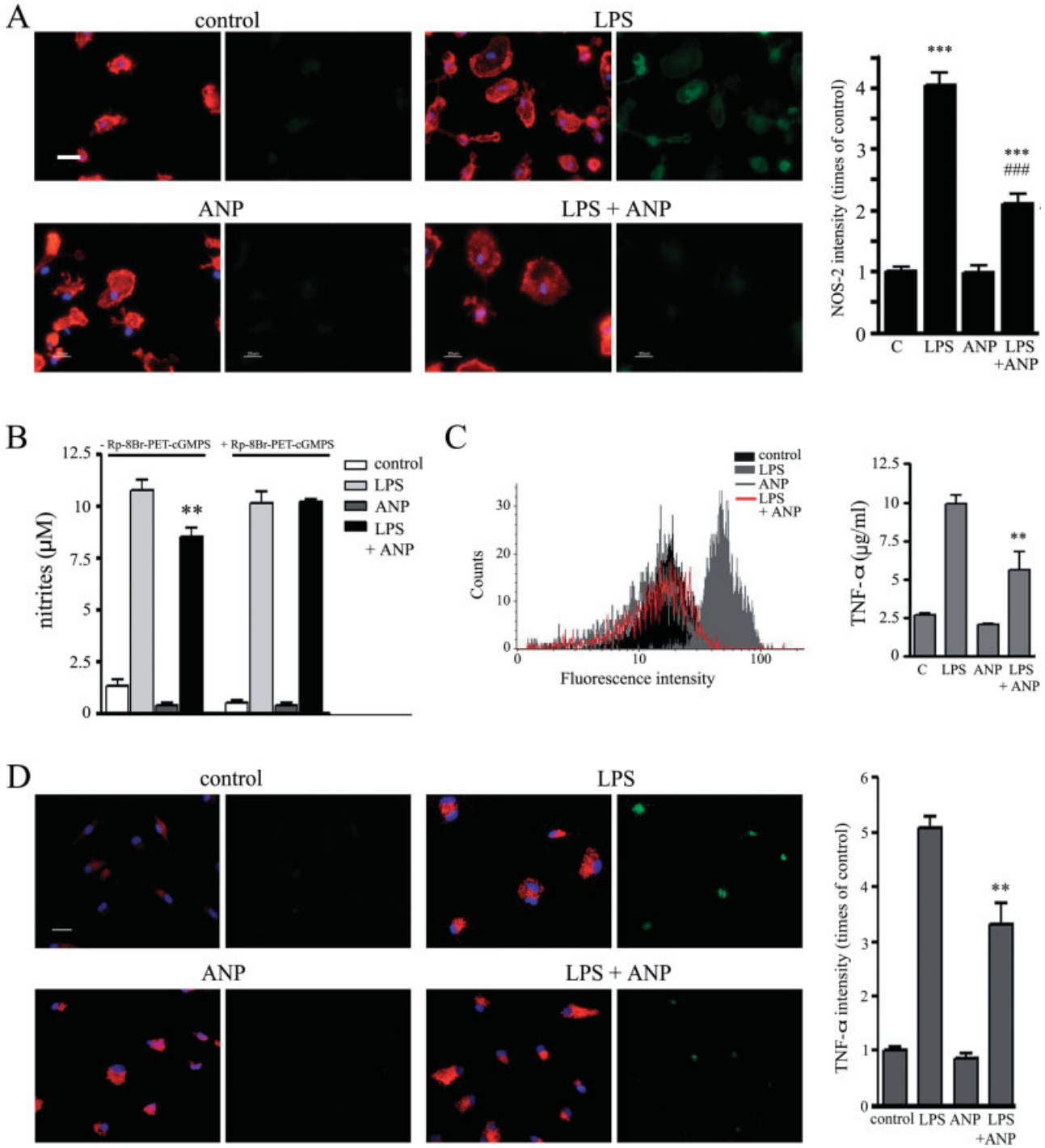

Fig. 9. Effect of ANP on LPS-induced NOS-2 and TNF-α in microglial cultures. (**A**) Cells untreated (control) or treated with LPS (100 ng/mL), ANP (1 μM) or both for 24 h were fixed and stained for NOS-2 (green) and F-actin (red). Scale bar, 25 μm (left). Quantification of NOS-2 fluorescence intensity was performed as in Fig. 8. Statistically significant differences versus control: $^{***}P < 0.001$ and versus LPS treatment: $^{\#\#\#}P < 0.001$. (**B**) Nitrite accumulation was determined in the incubation media after 48 h. In some cultures, the PKG inhibitor Rp-8Br-PET-cGMPS (0.5 μM) was preincubated for 1 h. Results are means ± SEM of three different experiments. $^{**}P < 0.01$: statistically significant difference evaluated by two-way ANOVA followed by Bonferroni's *post hoc* test respect to LPS treatment. (**C**) Representative cytometric analysis of TNF-α levels determined in the incubation media after 24 h in cultures treated as in A (left). Quantification shows means ± SEM of three different experiments (right). Significant difference versus LPS treatment: $^{**}P < 0.01$. (**D**) Staining for TNF-α (green), CD68 (red) and DAPI (blue) in cultures treated as in A. Scale bar, 25 μm (left). Quantification shows means ± SEM of three different experiments (right). Statistically significant differences versus LPS: $^{**}P < 0.01$. Except for B, statistically significant differences were evaluated by one-way ANOVA followed by Turkey's *post hoc* test. [Color figure can be viewed in the online issue, which is available at www.interscience.wiley.com.]

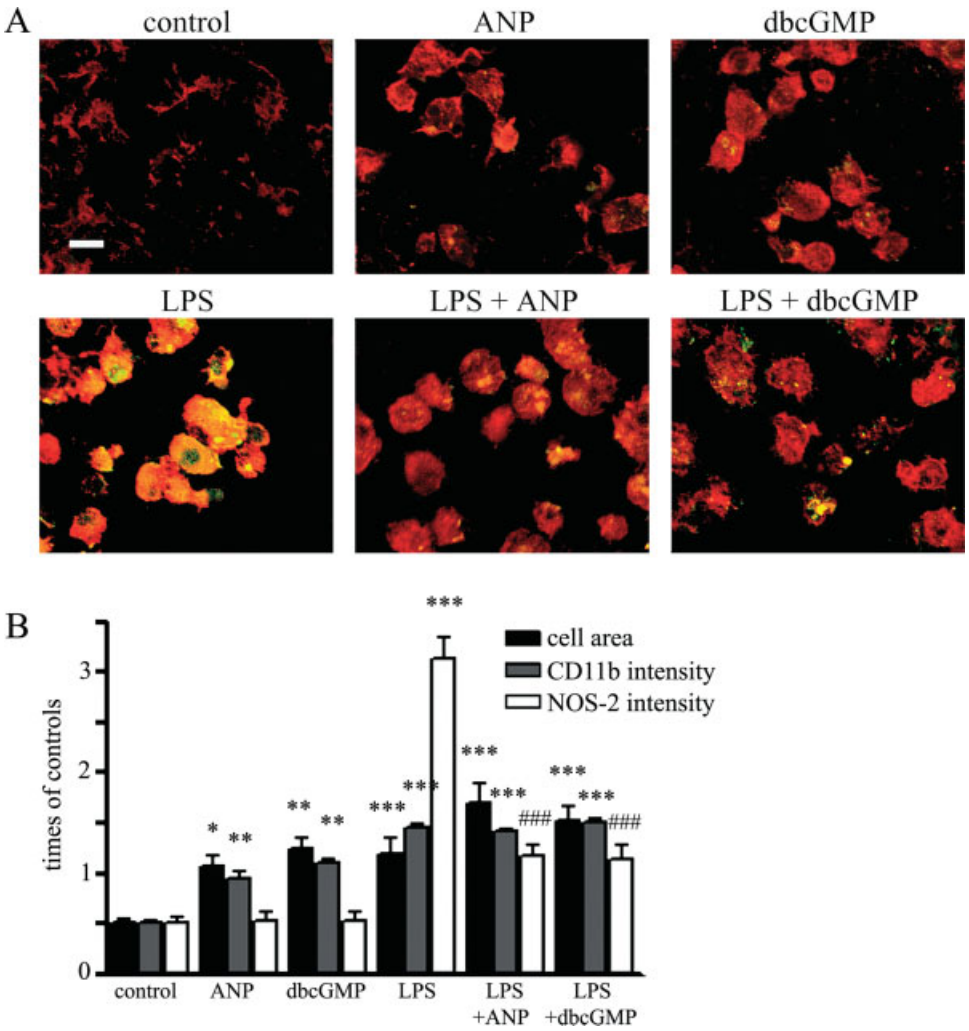

Fig. 10. Effect of ANP and dbcGMP on microglial morphology and CD11b and NOS-2 expression in organotypic cultures. (**A**) Hippocampal slice cultures were treated with LPS (1 μg/mL), ANP (1 μM), dbcGMP (100 μM) or with LPS and ANP or dbcGMP for 24 h. Then slices were double labeled for CD11b (red) and NOS-2 (green) and examined by confocal microscopy. Yellow labeling corresponds to CD11b- and NOS-2-positive microglial cells. Scale bar, 20 μm. (**B**) Quantification of microglial cell area (black bars) and CD11b (gray bars) and NOS-2 (white bars) fluorescence intensities in at least 100 cells in each experimental condition using MetaMorph Software (Version 6.1). Values are means ± SD and are expressed relative to controls. Statistically significant differences versus respective controls: $^{*}P < 0.05$; $^{**}P < 0.01$; $^{***}P < 0.001$; and versus LPS treatment: $^{\#\#\#}P < 0.001$ were evaluated by one-way ANOVA followed by Turkey's *post hoc* test in a representative experiment that was repeated with similar results.

primary cultures versus microglial cell lines. Differences between rat and mouse in the localization of components of the cGMP-signaling system have been described (van Staveren et al., 2004).

Cyclic GMP-mediated pathways have been implicated in the regulation of actin cytoskeleton and cell morphology in different cell types including macrophages (Boran and Garcia, 2007; Ke et al., 2001; Krepinsky et al., 2003; Sawada et al., 2001). However, previous studies failed to observe morphological changes elicited by dbcGMP in murine microglia co-cultured on a confluent monolayer of rat astrocytes (Kalla et al., 2003). Moreover, contrary to our observations ANP treatment was reported to suppress the LPS-induced shape change in rat microglial cultures (Moriyama et al., 2006). Differences in species or culture conditions may be responsible for these discrepancies. Most studies use microglia harvested by shaking mixed glial cultures, a procedure that yields cells with an amoeboid morphology, while we use primary microglia that remains attached to the culture dishes after lifting the astrocyte monolayer by mild trypsinization (Saura et al., 2003), and are maintained in isolated culture for only 2–3 days in the absence of serum. Furthermore, we observe similar cell shape changes in the microglia present in the astrocyte-enriched cultures and in organotypic cultures, conditions in which the microglial morphology is more like that of resting microglia in normal brain.

The effects of ANP and dbcGMP on the microglial actin cytoskeleton are potent (significant at 0.01 and 1 μM and maximal at 1 and 100 μM, respectively), very rapid (significant at 5 min and maximal at 30 min) and appear to involve PKG activation because they are prevented by the PKG inhibitor Rp-8Br-PET-cGMPS. A possible implication of PKA was ruled out by the lack of effect of its specific inhibitor Rp-cAMPS.

cGMP via PKG has been reported to regulate the activity and downstream effects of Rho GTPases (Pilz and Broderick, 2005). In this work, we show that the three mayor members of this family, RhoA, Rac, and Cdc42 are involved in the regulation by ANP of microglial actin cytoskeleton dynamics. We found that the Rho GTPase activator GGpp is able to prevent the ANP-induced morphological change in microglia suggesting that at least one of the Rho GTPases is inhibited by ANP. The observation that Y-27632, an inhibitor of ROCK, induced cell

rounding similarly to ANP or dbcGMP, and that addition of increasing concentrations of ANP to Y-27632 treated-cells caused a concomitant increment in lamellipodia and filopodia formation, a phenomenon known to involve Rac and Cdc42 activation (Hall, 1998), led us to hypothesize that the cGMP effects involved RhoA inhibition and Rac and Cdc42 activation. This hypothesis was confirmed by results from transfection assays with a constitutively active mutant of RhoA (V14RhoA) and dominant negative mutants of Rac and Cdc42 (N17Rac1 and N17Cdc42). In microglia transfected with these mutants, ANP was unable to induce rounding or formation of lamellipodia or filopodia, respectively. In contrast, nontransfected cells in the same culture dishes showed similar actin cytoskeletal changes in response to ANP as control cells. Inhibition of RhoA activity by cGMP-mediated pathways has been shown in different cell types (Gudi et al., 2002; Krepinsky et al., 2003; Sandu et al., 2001; Sauzeau et al., 2000; Sawada et al., 2001) and we recently described this effect in astrocytes (Boran and Garcia, 2007). Phosphorylation by PKG in Ser^{188} was reported to inhibit RhoA activity *in vitro* (Sauzeau et al., 2000; Sawada et al., 2001) and in smooth muscle cells the NO-cGMP pathway has been implicated in the inhibition of RhoA isoprenylation, a critical event for its membrane translocation and activation (Begum et al., 2002). Furthermore, in endothelial cells ANP has been reported to activate Rac (Furst et al., 2005) and PKG to phosphorylate the protein effector of Rac and Cdc42, p21-activated kinase (Pak)1, a relevant step for the regulation of cell morphology (Fryer et al., 2006). Whether any of these mechanisms operates in microglial cells is unknown at present.

Rho GTPases and their downstream effectors play crucial roles in regulating the actin rearrangements mediating different types of particle engulfment by phagocytic cells (Caron and Hall, 1998; Cox et al., 1997; Leverrier and Ridley, 2001; Massol et al., 1998). Dominant inhibitory variants of Rac and Cdc42 have been shown to inhibit FcγR-mediated phagocytosis (Caron and Hall, 1998; Massol et al., 1998) while specific inhibition of Rho was shown to block complement-, but not FcγR-mediated phagocytosis in one study (Caron and Hall, 1998 and to prevent FcγR-mediated phagocytosis in another (Hackam et al., 1997). In contrast, engulfment of apoptotic cells requires Rac and Cdc42 but it is blocked by activation of endogenous RhoA or overexpression of constitutively active RhoA (Leverrier and Ridley, 2001; Tosello-Trampont et al., 2003). Results presented here indicate that the mechanism underlying ANP-induced phagocytosis in microglia resembles that of apoptotic cell uptake. We show that microglia overexpressing constitutively active RhoA is not able to engulf inert particles when stimulated with ANP, indicating that inhibition of RhoA is a necessary event. Furthermore, overexpression of dominant negative Rac1 or Cdc42 reduced the ANP effect supporting their contribution to the phagocytic mechanism. In agreement with this, incubation with the general Rho GTPase activator GGpp prevented particle uptake in the absence, but not in the presence, of an inhibitor of ROCK, further implicating this RhoA effector in the negative regulation of the phagocytic response.

In macrophages, while FcγR-mediated phagocytosis is accompanied by release of proinflammatory mediators, complement-mediated phagocytosis does not initiate a proinflammatory response and apoptotic cell ingestion is anti-inflammatory (Aderem and Underhill, 1999; Erwig and Henson, 2007). In macrophages, ANP was shown to increase ingestion of opsonized particles and to enhance reactive oxygen production (Vollmar et al., 1997). However, it decreased the expression of the typical proinflammatory genes NOS-2 and TNF-α (Vollmar, 2005). In this work, we also observed that ANP does not induce NOS-2 or TNF-α expression in microglia and, on the contrary, is able to significantly decrease their induction by LPS. Additionally, we did not observe increases in reactive oxygen species measured by DCFH (2′,7′-dichlorofluorescein) oxidation in microglia stimulated with ANP (not shown). These results also support the hypothesis that in microglia ANP promotes a response with characteristics similar to those reported for clearance of apoptotic cells by phagocytes. In agreement with our results, a recent report showed inhibition by ANP of nitrite accumulation and IL-1β expression in rat microglial cultures (Moriyama et al., 2006) and previous studies in the mouse microglial cell line N9 had shown that cGMP generating compounds opposed LPS-induced microglial TNF-α release (Paris et al., 2000) and Aβ-amyloid-induced leukotriene B4 release (Paris et al., 1999). In contrast, enhanced basal and LPS-induced secretion of TNF-α and IL-1β and expression of NOS-2 and MHC II have been reported in rat microglial cells treated for 24 h with zaprinast, an inhibitor of cGMP-selective phosphodiesterases, or with 1 mM dbcGMP (Choi et al., 2002). These conditions are expected to maintain cGMP levels elevated for longer periods of time than in our study where exposure to ANP will only transiently increase cGMP (Baltrons et al., 1997), and could lead to activation of the cAMP-PKA pathway also known to affect microglial morphology and inflammatory gene expression (Dello Russo et al., 2004; Feinstein et al., 2002; Kalla et al., 2003). In contrast, in hippocampal organotypic cultures treated with ANP or dbcGMP we have observed increased expression of the surface marker CD11b, an integrin molecule implicated in the morphological changes that occur in microglia during inflammation progression (Gonzalez-Scarano and Baltuch, 1999). A recent study also showed the involvement of the cGMP-PKG-CREB pathway in up-regulating CD11b in a mouse microglial cell line (Roy et al., 2006). However, in CD11b-positive cells in the organotypic cultures, ANP or dbcGMP decreased LPS-induced NOS-2 expression, indicating that cGMP can have opposite regulatory effects on the expression of different inflammatory genes in microglial cells.

As reviewed by Town et al. (2005), activation of microglia in response to brain injury involves a continuum spectrum of phenotypes rather than one simple stage. Microglia activation oscillates between two end-points

depending on the stimulatory environment, one corresponds to the innate activation (with phagocytic phenotype and anti-inflammatory cytokine secretion) and the other is the adaptive activation (with release of proinflammatory cytokines) that is associated with CD40 co-stimulation. According to that scheme, our results suggest that ANP stimulation of the cGMP-PKG pathway induces a microglial phenotype that is closer to the first end-point. This microglial activation stage does not seem to be deleterious for the tissue, as shown in microglial cells challenged with Aβ or apoptotic cells in the absence of CD40 signaling (Minghetti et al., 2005; Townsend et al., 2005).

Evidence from macrophages indicates that beneficial effects of ANP in ischemic injury may result in part from its ability to inhibit activation of inflammatory cells (Vollmar, 2005). In these cells, ANP regulates activity in an autocrine manner (Kiemer and Vollmar, 1998). A recent report showing expression of mRNA for ANP, and its receptors in microglial cells suggests that ANP may also be an autocrine regulator in these cells (Moriyama et al., 2006). NPs have been localized at the mRNA and protein level in neurons and astrocytes (Wiggins et al., 2003; Zamir et al., 1986) and release from astrocytes shown to occur by a calcium-dependent process (Krzan et al., 2003). Thus, paracrine effects of NPs in microglia are also possible. Very little is known about the role of NPs in brain tissue under normal or pathological conditions. Increased cGMP-immunoreactivity after stimulation with ANP has been found in brain blood vessels (de Vente and Steinbusch, 2000) suggesting a role for NPs in the regulation of cerebral blood flow as occurs outside the blood brain barrier. Additionally, brain ANP content was reported to increase in reactive glial cells surrounding experimental brain infarction (Nogami et al., 2001) and the ANP-cGMP system to be up-regulated during cortical spreading depression (CSD) suggesting that it may contribute to CSD-induced protection against ischemic insult (Wiggins et al., 2003). Results shown here, suggest that additional beneficial effects of ANP in the damaged brain tissue may result from stimulation of microglial phagocytic activity and down-regulation of inflammatory gene expression.

ACKNOWLEDGMENTS

M.S. Borán is the recipient of a predoctoral fellowship from AGAUR, Generalitat de Catalunya. The authors thank Drs. A. Ridley (UCL, London, UK) and C. Guerri (CIPF, Valencia, Spain) for providing mutant Rho GTPase plasmids and Dr. J. de Vente (Maastricht University, The Nederlands) for donating anti-sheep cGMP antibody. They also thank Cristina Gutierrez for assistance in cell cultures and Manuela Costa for support in cytometric measurements (UAB, Barcelona, Spain).

REFERENCES

abd-el-Basset E, Fedoroff S. 1995. Effect of bacterial wall lipopolysaccharide (LPS) on morphology, motility, and cytoskeletal organization of microglia in cultures. J Neurosci Res 41:222–237.

Abraham H, Losonczy A, Czeh G, Lazar G. 2001. Rapid activation of microglial cells by hypoxia, kainic acid, and potassium ions in slice preparations of the rat hippocampus. Brain Res 906:115–126.

Aderem A, Underhill DM. 1999. Mechanisms of phagocytosis in macrophages. Annu Rev Immunol 17:593–623.

Agullo L, Baltrons MA, Garcia A. 1995. Calcium-dependent nitric oxide formation in glial cells. Brain Res 686:160–168.

Allen WE, Jones GE, Pollard JW, Ridley AJ. 1997. Rho, Rac and Cdc42 regulate actin organization and cell adhesion in macrophages. J Cell Sci 110(Part 6):707–720.

Aloisi F. 2001. Immune function of microglia. Glia 36:165–179.

Baltrons MA, Garcia A. 1999. Nitric oxide-independent down-regulation of soluble guanylyl cyclase by bacterial endotoxin in astroglial cells. J Neurochem 73:2149–2157.

Baltrons MA, Saadoun S, Agullo L, Garcia A. 1997. Regulation by calcium of the nitric oxide/cyclic GMP system in cerebellar granule cells and astroglia in culture. J Neurosci Res 49:333–341.

Begum N, Sandu OA, Duddy N. 2002. Negative regulation of rho signaling by insulin and its impact on actin cytoskeleton organization in vascular smooth muscle cells: Role of nitric oxide and cyclic guanosine monophosphate signaling pathways. Diabetes 51:2256–2263.

Bohatschek M, Kloss CU, Kalla R, Raivich G. 2001. In vitro model of microglial deramification: Ramified microglia transform into amoeboid phagocytes following addition of brain cell membranes to microglia-astrocyte cocultures. J Neurosci Res 64:508–522.

Boran MS, Garcia A. 2007. The cyclic GMP-protein kinase G pathway regulates cytoskeleton dynamics and motility in astrocytes. J Neurochem 102:216–230.

Caron E, Hall A. 1998. Identification of two distinct mechanisms of phagocytosis controlled by different Rho GTPases. Science 282:1717–1721.

Choi SH, Choi DH, Song KS, Shin KH, Chun BG. 2002. Zaprinast, an inhibitor of cGMP-selective phosphodiesterases, enhances the secretion of TNF-α and IL-1β and the expression of iNOS and MHC class II molecules in rat microglial cells. J Neurosci Res 67:411–421.

Cox D, Chang P, Zhang Q, Reddy PG, Bokoch GM, Greenberg S. 1997. Requirements for both Rac1 and Cdc42 in membrane ruffling and phagocytosis in leukocytes. J Exp Med 186:1487–1494.

de Vente J, Bol JG, Steinbusch HW. 1989. Localization of cGMP in the cerebellum of the adult rat: An immunohistochemical study. Brain Res 504:332–337.

de Vente J, Steinbusch H. 2000. Nitric oxide-cGMP signalling in the rat brain. In: Steinbusch H, de Vente J, Vicent S, editors. Funcional neuroanatomy of the nitric oxide system. Handbook of chemical neuroanatomy. Amsterdam: Elservier. pp 355– 415.

Dello Russo C, Boullerne AI, Gavrilyuk V, Feinstein DL. 2004. Inhibition of microglial inflammatory responses by norepinephrine: Effects on nitric oxide and interleukin-1β production. J Neuroinflammation 1:9.

Diaz-Cazorla M, Perez-Sala D, Lamas S. 1999. Dual effect of nitric oxide donors on cyclooxygenase-2 expression in human mesangial cells. J Am Soc Nephrol 10:943–952.

Erwig LP, Henson PM. 2007. Clearance of apoptotic cells by phagocytes. Cell Death Differ. In press. Epub ahead of print (doi:10.1038/sj.ccd.4402184).

Etienne-Manneville S, Hall A. 2002. Rho GTPases in cell biology. Nature 420:629–635.

Feinstein DL, Heneka MT, Gavrilyuk V, Dello Russo C, Weinberg G, Galea E. 2002. Noradrenergic regulation of inflammatory gene expression in brain. Neurochem Int 41:357–365.

Fryer BH, Wang C, Vedantam S, Zhou GL, Jin S, Fletcher L, Simon MC, Field J. 2006. cGMP-dependent protein kinase phosphorylates p21-activated kinase (Pak) 1, inhibiting Pak/Nck binding and stimulating Pak/vasodilator-stimulated phosphoprotein association. J Biol Chem 281:11487–11495.

Furst R, Brueckl C, Kuebler WM, Zahler S, Krotz F, Gorlach A, Vollmar AM, Kiemer AK. 2005. Atrial natriuretic peptide induces mitogen-activated protein kinase phosphatase-1 in human endothelial cells via Rac1 and NAD(P)H oxidase/Nox2-activation. Circ Res 96:43–53.

Galea E, Feinstein DL, Reis DJ. 1992. Induction of calcium-independent nitric oxide synthase activity in primary rat glial cultures. Proc Natl Acad Sci USA 89:10945–10949.

Ghafouri M, Amini S, Khalili K, Sawaya BE. 2006. HIV-1 associated dementia: Symptoms and causes. Retrovirology 3:28.

Gonzalez-Scarano F, Baltuch G. 1999. Microglia as mediators of inflammatory and degenerative diseases. Annu Rev Neurosci 22:219–240.

Gudi T, Chen JC, Casteel DE, Seasholtz TM, Boss GR, Pilz RB. 2002. cGMP-dependent protein kinase inhibits serum-response element-dependent transcription by inhibiting rho activation and functions. J Biol Chem 277:37382–37393.

Hackam DJ, Rotstein OD, Schreiber A, Zhang W, Grinstein S. 1997. Rho is required for the initiation of calcium signaling and phagocytosis by Fcγ receptors in macrophages. J Exp Med 186:955–966.

Hall A. 1998. Rho GTPases and the actin cytoskeleton. Science 279:509–514.
Howard TH, Oresajo CO. 1985. A method for quantifying F-actin in chemotactic peptide activated neutrophils: Study of the effect of tBOC peptide. Cell Motil 5:545–557.
Kalla R, Bohatschek M, Kloss CU, Krol J, Von Maltzan X, Raivich G. 2003. Loss of microglial ramification in microglia-astrocyte cocultures: Involvement of adenylate cyclase, calcium, phosphatase, and Gi-protein systems. Glia 41:50–63.
Ke X, Terashima M, Nariai Y, Nakashima Y, Nabika T, Tanigawa Y. 2001. Nitric oxide regulates actin reorganization through cGMP and Ca(2+)/calmodulin in RAW 264.7 cells. Biochim Biophys Acta 1539: 101–113.
Kiemer AK, Vollmar AM. 1998. Autocrine regulation of inducible nitric-oxide synthase in macrophages by atrial natriuretic peptide. J Biol Chem 273:13444–13451.
Kim SU, de Vellis J. 2005. Microglia in health and disease. J Neurosci Res 81:302–313.
Kim YS, Joh TH. 2006. Microglia, major player in the brain inflammation: Their roles in the pathogenesis of Parkinson's disease. Exp Mol Med 38:333–347.
Kloss CU, Bohatschek M, Kreutzberg GW, Raivich G. 2001. Effect of lipopolysaccharide on the morphology and integrin immunoreactivity of ramified microglia in the mouse brain and in cell culture. Exp Neurol 168:32–46.
Krepinsky JC, Ingram AJ, Tang D, Wu D, Liu L, Scholey JW. 2003. Nitric oxide inhibits stretch-induced MAPK activation in mesangial cells through RhoA inactivation. J Am Soc Nephrol 14:2790–2800.
Krzan M, Stenovec M, Kreft M, Pangrsic T, Grilc S, Haydon PG, Zorec R. 2003. Calcium-dependent exocytosis of atrial natriuretic peptide from astrocytes. J Neurosci 23:1580–1583.
Leverrier Y, Ridley AJ. 2001. Requirement for Rho GTPases and PI 3-kinases during apoptotic cell phagocytosis by macrophages. Curr Biol 11:195–199.
Mackay DJ, Hall A. 1998. Rho GTPases. J Biol Chem 273:20685–20688.
Massol P, Montcourrier P, Guillemot JC, Chavrier P. 1998. Fc receptor-mediated phagocytosis requires CDC42 and Rac1. EMBO J 17:6219–6229.
Minghetti L, Ajmone-Cat MA, De Berardinis MA, De Simone R. 2005. Microglial activation in chronic neurodegenerative diseases: Roles of apoptotic neurons and chronic stimulation. Brain Res Brain Res Rev 48:251–256.
Moriyama N, Taniguchi M, Miyano K, Miyoshi M, Watanabe T. 2006. ANP inhibits LPS-induced stimulation of rat microglial cells by suppressing NF-κB and AP-1 activations. Biochem Biophys Res Commun 350:322–328.
Nimmerjahn A, Kirchhoff F, Helmchen F. 2005. Resting microglial cells are highly dynamic surveillants of brain parenchyma in vivo. Science 308:1314–1318.
Nogami M, Shiga J, Takatsu A, Endo N, Ishiyama I. 2001. Immunohistochemistry of atrial natriuretic peptide in brain infarction. Histochem J 33:87–90.
Paris D, Town T, Mullan M. 2000. Novel strategies for opposing murine microglial activation. Neurosci Lett 278:5–8.
Paris D, Town T, Parker TA, Tan J, Humphrey J, Crawford F, Mullan M. 1999. Inhibition of Alzheimer's β-amyloid induced vasoactivity and proinflammatory response in microglia by a cGMP-dependent mechanism. Exp Neurol 157:211–221.
Perez-Sala D, Cernuda-Morollon E, Diaz-Cazorla M, Rodriguez-Pascual F, Lamas S. 2001. Posttranscriptional regulation of human iNOS by the NO/cGMP pathway. Am J Physiol Renal Physiol 280:F466–F473.
Pilz RB, Broderick KE. 2005. Role of cyclic GMP in gene regulation. Front Biosci 10:1239–1268.
Potucek YD, Crain JM, Watters JJ. 2006. Purinergic receptors modulate MAP kinases and transcription factors that control microglial inflammatory gene expression. Neurochem Int 49:204–214.
Raivich G, Jones LL, Werner A, Bluthmann H, Doetschmann T, Kreutzberg GW. 1999. Molecular signals for glial activation: Pro- and anti-inflammatory cytokines in the injured brain. Acta Neurochir Suppl 73:21–30.
Roy A, Fung YK, Liu X, Pahan K. 2006. Up-regulation of microglial CD11b expression by nitric oxide. J Biol Chem 281:14971–14980.
Sandu OA, Ito M, Begum N. 2001. Selected contribution: Insulin utilizes NO/cGMP pathway to activate myosin phosphatase via Rho inhibition in vascular smooth muscle. J Appl Physiol 91:1475–1482.
Saura J, Tusell JM, Serratosa J. 2003. High-yield isolation of murine microglia by mild trypsinization. Glia 44:183–189.
Sauzeau V, Le Jeune H, Cario-Toumaniantz C, Smolenski A, Lohmann SM, Bertoglio J, Chardin P, Pacaud P, Loirand G. 2000. Cyclic GMP-dependent protein kinase signaling pathway inhibits RhoA-induced Ca2+ sensitization of contraction in vascular smooth muscle. J Biol Chem 275:21722–21729.
Sauzeau V, Rolli-Derkinderen M, Marionneau C, Loirand G, Pacaud P. 2003. RhoA expression is controlled by nitric oxide through cGMP-dependent protein kinase activation. J Biol Chem 278:9472–9480.
Sawada N, Itoh H, Yamashita J, Doi K, Inoue M, Masatsugu K, Fukunaga Y, Sakaguchi S, Sone M, Yamahara K, Yurugi T, Nakao K. 2001. cGMP-dependent protein kinase phosphorylates and inactivates RhoA. Biochem Biophys Res Commun 280:798–805.
Sola C, Casal C, Tusell JM, Serratosa J. 2002. Astrocytes enhance lipopolysaccharide-induced nitric oxide production by microglial cells. Eur J Neurosci 16:1275–1283.
Stoppini L, Buchs PA, Muller D. 1991. A simple method for organotypic cultures of nervous tissue. J Neurosci Methods 37:173–182.
Streit WJ. 2005. Microglia and neuroprotection: Implications for Alzheimer's disease. Brain Res Brain Res Rev 48:234–239.
Streit WJ, Kreutzberg GW. 1988. Response of endogenous glial cells to motor neuron degeneration induced by toxic ricin. J Comp Neurol 268:248–263.
Teunissen CE, Steinbusch HW, Markerink-van Ittersum M, De Bruijn C, Axer H, De Vente J. 2000. Whole brain spheroid cultures as a model to study the development of nitric oxide synthase-guanylate cyclase signal transduction. Brain Res Dev Brain Res 125:99–115.
Tosello-Trampont AC, Nakada-Tsukui K, Ravichandran KS. 2003. Engulfment of apoptotic cells is negatively regulated by Rho-mediated signaling. J Biol Chem 278:49911–49919.
Town T, Nikolic V, Tan J. 2005. The microglial "activation" continuum: From innate to adaptive responses. J Neuroinflammation 2:24.
Townsend KP, Town T, Mori T, Lue LF, Shytle D, Sanberg PR, Morgan D, Fernandez F, Flavell RA, Tan J. 2005. CD40 signaling regulates innate and adaptive activation of microglia in response to amyloid β-peptide. Eur J Immunol 35:901–910.
van Staveren WC, Steinbusch HW, Markerink-van Ittersum M, Behrends S, de Vente J. 2004. Species differences in the localization of cGMP-producing and NO-responsive elements in the mouse and rat hippocampus using cGMP immunocytochemistry. Eur J Neurosci 19:2155–2168.
Vollmar AM. 2005. The role of atrial natriuretic peptide in the immune system. Peptides 26:1086–1094.
Vollmar AM, Forster R, Schulz R. 1997. Effects of atrial natriuretic peptide on phagocytosis and respiratory burst in murine macrophages. Eur J Pharmacol 319:279–285.
Wiggins AK, Shen PJ, Gundlach AL. 2003. Atrial natriuretic peptide expression is increased in rat cerebral cortex following spreading depression: Possible contribution to sd-induced neuroprotection. Neuroscience 118:715–726.
Wyss-Coray T. 2006. Inflammation in Alzheimer disease: Driving force, bystander or beneficial response? Nat Med 12:1005–1015.
Zamir N, Skofitsch G, Eskay RL, Jacobowitz DM. 1986. Distribution of immunoreactive atrial natriuretic peptides in the central nervous system of the rat. Brain Res 365:105–111.